Thermomechanical Problems in Fusion Reactor Blankets

M. A. Abdou, M. S. Tillack and A. R. Raffray

Mechanical, Aerospace and Nuclear Engineering Department
University of California-Los Angeles
Los Angeles, California, USA 90024

ABSTRACT

Liquid Metals and solid breeders are candidates for use in fusion reactor blankets. Both types of blankets have major advantages. However, there are critical issues that can severly limit their potential economic, safety and environmental advantages. This paper focuses on those key issues that are related to thermo-mechanical performance of liquid metal and solid breeder blankets. The primary material and configuration design options are described. The key thermomechanical issues are elucidated, and, in many cases, quantified. Recent progress in model developments and experiments is summarized.

1. INTRODUCTION

The economic, safety and environmental attractiveness of future fusion reactors will be determined, to a large extent, by the choice of materials for and the performance of the blanket. The primary objectives of the blanket are: 1) to convert the kinetic energy of fusion neutrons and secondary gamma rays into heat, and 2) to breed tritium at a rate adequate for attaining tritium fuel self sufficiency. The blanket is exposed to an intense radiation environment. Radioactivity and associated decay heat can be produced in the structure, breeder, multiplier coolant, and other blanket components. Hence, material choices have large impact on safety and environmental impact. The unique combination of conditions in the fusion environment such as intense radiation, strong magnetic field and vacuum as well as the requirements for high temperature operation to improve economics and temperature control to influence tritium transport, make the design of the blanket a challenging task.

Liquid metals and solid breeders are the primary concepts being considered in fusion programs around the world. Other concepts such as molten salts and aquious solutions have been proposed but they are much less favored than the primary options.

Liquid metal and solid breeder blankets have major advantages. However, there are critical issures that can seriously limit their economic, safety, and environmental potential. This paper is concerned with an important subset of those issues; namely the key issues related to the thermomechanical behavior of the blanket. Both liquid metal and solid breeder blankets are addressed. The primary materials and configuration design options are described. The key thermomechanical problems are elucidated, and, in many cases, quantified. Recent progress in analytical and numerical model development and in experiments is summarized. Priority items for future R & D are indicated.

2. Liquid Metal Blankets and High-Heat-Flux Components

2.1 Introduction

Liquid metals are potential candidates for both the breeding material and coolant in blankets and high heat flux components such as divertors and limiters. As breeders, pure lithium or the eutectic $Li_{17}Pb_{83}$ have high potential tritium breeding ratios. As coolants, liquid metals have good heat removal capabilities and can operate at high temperature, allowing for efficient power conversion. Other significant advantages include negligible radiation damage to the breeder, flexible operating conditions, and overall design simplicity. In addition, liquid metals have recently been proposed as a protective medium to reduce the problems of erosion, heat removal, and radiation damage in high heat flux components (HHFC).

However, a number of problems and uncertainties limit the attractiveness of liquid metal components. These are listed in Table 1, and discussed in detail in [1]. Magnetohydrodynamic (MHD) effects are unique to liquid metals, and serve to reduce the thermal-hydraulic performance by greatly increasing the pressure drop and reducing the heat transfer coefficient through laminarization of the flow. Material interactions lead to limitations on allowable operating temperatures, and the potential effects of chemical reactions under accident scenarios may lead to restrictions in the use of liquid metals – particularly pure lithium. Overall, large uncertainties in the thermomechanical behavior of liquid metal components make it difficult to ensure adequate performance [2].

During recent years, efforts thoughout the world have provided improved understanding of the thermomechanical problems of liquid metal components and the development of design solutions.
Substantial progress has been made in modeling and understanding MHD fluid flow and pressure drop in laminar duct flow. Numerical models have been developed to provide the capability to analyze more complex geometries than earlier analytic techniques. Both numerical and analytic solutions have been obtained in a number of simple geometries for both conducting and insulating ducts. Other areas of recent activity include non-laminar, two-phase, and free surface flow with liquid metals.

New design solutions have evolved in an attempt to exploit the benefits and reduce the problems inherent to liquid metals. Examples of these include, for example: MHD flow tailoring, innovative use of insulating materials, two-phase Li/He flow, and novel power conversion systems. These are discussed in more detail in Section 2.4.

Table 1. Generic Liquid Metal Blanket Issues

Tritium fuel self-sufficiency
Magnetohydrodynamic effects
fluid flow and pressure drop
heat transfer
Material interactions
corrosion/mass transport
chemical reactions
Structural response in the fusion environment
irradiation effects on material properties
response to complex loading conditions
failure modes
Tritium recovery and control

Experimental data have been scarce, but are making a large impact. For example, observations of fluctuations in the flow may lead to substantial enhancements in heat transfer coefficients. Corrosion experiments have provided data to better define the operating limits and to provide insight into the dominant processes, which will help to design systems which minimize the negative impacts. These new developments have improved the potential of liquid metal systems as candidates for use in future fusion reactors.

2.2 Design Options

A. Blankets

Research and conceptual design studies over the past 15 years have led to the adoption of a limited set of material choices for liquid metal blankets. These are listed in Table 2. The exact choice of materials involves a complex set of trade-offs, involving different issues and design strategies. Each combination of materials implies a unique set of issues.

An even wider variety of choices exists in defining a configuration that results in optimum performance. For blankets, the two major classes of designs are self-cooled and separately-cooled. Separately-cooled designs use stagnant or slow-flowing liquid metal breeder with either water or helium coolant. The most prominent candidate at this time is a water-cooled $Li_{17}Pb_{83}$ blanket [3]. Figure 1 shows a NET design which contains water coolant tubes running through the breeder, all encased in a circular U-tube [3].

Table 2. Liquid Metal Component Material Options

Breeders	Li, $Li_{17}Pb_{83}$
Coolants ($Li_{17}Pb_{83}$ only)	self, He, H_2O
Structural materials	stainless steel, V-alloy
Protective films	Li, Ga, Sn (HHFC)

The issues for separately cooled designs are generally similar to self-cooled designs, except for the reduction or elimination of MHD problems (at the expense of tritium breeding capability, material compatibility, and design complexity). In this paper, the thermomechanics of self-cooled designs will be examined as representative of the entire class of liquid metal blankets.

A number of self-cooled blanket designs are described in [4,5,42]. Self-cooled blankets use the liquid metal simultaneously as breeder and coolant. Both Li and $Li_{17}Pb_{83}$ have been proposed in a variety of configurations. Previous designs, such as the BCSS toroidal/poloidal flow concept, attempted to alleviate MHD problems by incorporating relatively complex flow paths, including bends, manifolding, orifices, etc. Figure 2 shows a schematic of the BCSS design [42]. More recently, a self-cooled NET design has been proposed with similar features (see Fig. 3) [8].

Some recent designs attempt to resolve MHD problems using simpler flow paths and structure geometries. These "advanced" designs rely on techniques such as flow channel inserts or "flow tailoring", as described in Section 2.4. For example, Fig. 4 shows a cross section of a TPSS design which uses simple straight flow paths [13]. These simpler designs are expected to provide higher reliability and more predictable thermal-hydraulic characteristics.

B. High Heat Flux Components (HHFC)

Two important and different concerns have led to the consideration of liquid metals for high heat flux components such as divertors and limiters. First, safety concerns over the use of water-cooled components in a reactor with lithium-containing blankets make it highly desirable to provide a viable non-water coolant. Second, the design margin and lifetime of diverors and limiters are currently very small. This limitation on the lifetime is caused by the rapid erosion of solid materials on the plasma side of divertors and limiters. Liquid metal films on the plasma side of limiters and divertors can protect the solid material. Designs for renewable liquid metal films have been developed and can potentially extend the lifetime of diver-

tors/limiters. Furthermore, the liquid metal film may possibly remove a large part of the heat load.

Designs with liquid metal coolants in closed configurations closely resemble designs using water. Extra attention is given to the flow paths to align the flow direction with the magnetic field to the maximum extent possible. Even then, the use of efficient insulating coatings is necessary to achieve even moderate design windows (in the range of 5–10 MW/m^2 surface heat flux removal) [6].

Free surface configurations offer the possibility of removing surface heat fluxes of 30 MW/m^2 or more. If plasma contamination can be avoided, liquid metal protecton could extend the lifetime of high heat flux components considerably.as. The most promising liquid metals are Li, Ga and Sn. Many design variations have been proposed [7,8,9]. These are summarized in Table 3.

Table 3. Options for Free Surface Contact Devices

Continuous Films
Free-falling film
Pumped film
Droplets
Droplet cloud
Electromagnetic droplet jet

2.3 Description of thermomechanical issues

Several of the prevailing issues for liquid metal components are interlinked by simultaneous design constraints on allowable temperatures and stresses. These issues are generically referred to as "thermomechanical" issues. They include thermal-hydraulics, material interactions (which set temperature limits), and structural mechanics.

To understand the interrelationship between these issues, consider a simplified design consisting of a single straight duct heated by a surface heat flux and bulk heating, with the coolant entering from the bottom and exiting from the top (see Fig. 5).

Figure 5 Liquid Metal Coolant Duct

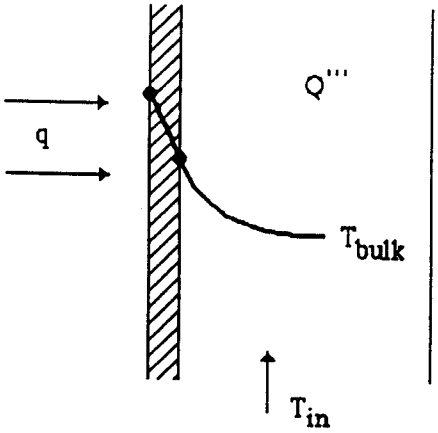

The MHD pressure gradient in a straight duct is given approximately by:

$$\nabla p = \sigma_f v B^2 \Phi \qquad \Phi = \frac{\sigma_w t}{\sigma_f a} \quad (1)$$

where σ_f is the fluid conductivity, v is the average velocity, B is the magnetic field strength perpendicular to the flow direction, and Φ is the wall conductance ratio – a nondimensional parameter comparing the electrical conductance of the wall to that of the fluid with (t) as the thickness of the wall and (a) is the duct dimension in the direction of the magnetic field.

In order to propel the fluid across the region of finite MHD pressure gradient, an external pressure head must be supplied. This results in relatively large pressures and pressure stress near the inlet to the coolant duct. The pressure stress is normally proportional to the ratio of duct width to wall thickness:

$$\sigma_p \sim \frac{\Delta p\, a}{t} \sim \sigma_w v B^2 L \qquad (2)$$

Notice, the pressure stress is independent of the channel dimensions: the only effective means to reduce stresses is to keep the velocity low.

However, the flow rate must be relatively high to remove heat adequately to maintain all the temperatures within material and structural limits. These limits arise from considerations of corrosion and mass transport, thermal stresses, and material behavior under irradiation, The peak structure temperature, T_s^m, is given by:

$$T_s^m = T_{in} + \Delta T_{bulk}(v) + \Delta T_{film}(v) + \Delta T_s \qquad (3)$$

where ΔT_{bulk},ΔT_{film} and ΔT, are the average temperature rise in the coolant bulk, coolant film and the structural wall, respectively.

The maximum temperature at the interface between the coolant and structure, T_{int}^{m}, is limited by corrosion considerations and is given by:

$$T_{int}^{m} = T_{in} + \Delta T_{bulk} + \Delta T_{film} \qquad (4)$$

Figure 6 shows a typical design window, which includes a maximum limit on flow speed due to pressure stresses and minimum limits to provide adequate cooling to maintain the peak structure and interface temperatures within design targets.

Figure 1. Example Design Window for a Li/V Blanket

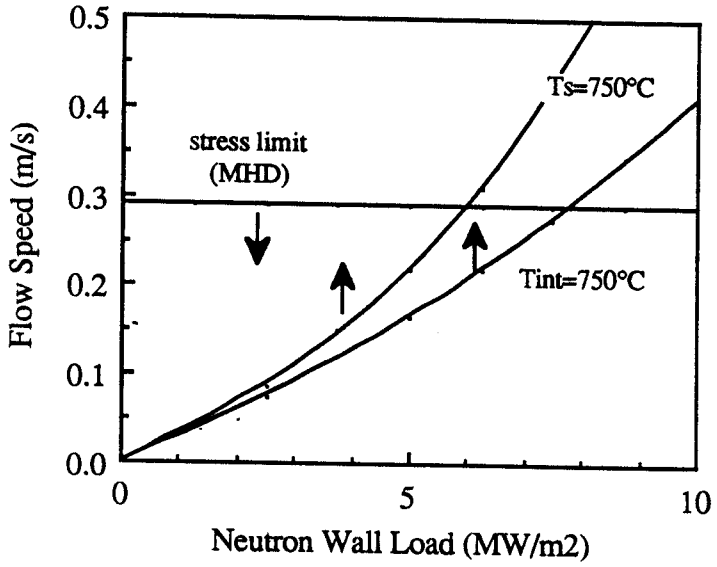

Uncertainties in the thermomechanical behavior of liquid metal components exacerbates this problem. The design window is based on imperfect understanding of both the physical phenomena as well as the appropriate design limits, so that components must be designed with additional margin to cover the uncertainties.

1. Fluid Flow and Thermal Performance Uncertainties. Prediction of MHD velocity profiles and pressure drop is difficult in actual reactor components. The predictive capabilities which exist today are limited to relatively simple geometries operating under idealized conditions. Large uncertainties remain in the MHD flow behavior of more complex components under three-dimensional magnetic fields, including effects due to the complex fusion environment (thermal and radiation-induced changes, transients, etc.). The velocity profiles are a particular concern, because small changes in geometry can lead to large changes in the velocity profile. The total pressure drop in many designs is less sensitive to local changes, and can be estimated with greater accuracy using simple correlations.

The velocity profiles are also important because they determine temperature profiles, which in turn affect most of the important phenomena in blankets and high heat flux components. Local features of the velocity profiles can directly influence the location and magnitude of hots spots, which usually determine operating limits.

2. Material interaction uncertainties. Liquid metals can interact strongly with the structural and containment materials, leading to corrosion and material properties degradation, and high mass transfer rates. The nature of the interaction depends very strongly on the exact material composition as well as the operating conditions, including temperature and impurity concentrations. Generally, higher temperatures result in higher interaction rates, such that this class of issues results in temperature limits of operation. Much work needs to be done to define the important reactions which govern the interactions, establish acceptable design limits, and develop methods to reduce the problems.

3. Structural mechanics uncertainties. Structural responses are very complex in liquid metal components, both because the loading conditions are strongly affected by MHD effects and because materials behavior in the fusion environment is largely unexplored. Limits on T_s^m and T_{int}^m are, therefore, uncertain.

The general design strategy for self-cooled blankets is shown in Figure 7. As described above, straight flow paths lead to unacceptably high pressure drop and/or high temperatures at the first wall. Design solutions require some combination of reduced pressure drop to allow higher flow speeds, or improved heat transfer coefficient. The most attractive methods to reduce the pressure drop include the use of flow paths parallel to the magnetic field (which generally implies manifolding and bends), reduction in wall conductance through the use of insulating materials, or reduction in the fluid conductivity using two-phase flow. Attractive methods to enhance heat transfer include flow profile control ("flow tailoring") or enhanced mixing. These methods to improve liquid metal blanket thermal-hydraulics are discussed in more detail in Section 2.4.

Free surface applications of liquid metals have their own unique set of issues. MHD issues are important for most designs concepts. The nature of free surface flow is substantially different from closed channel flow, and new issues arise, such as thickness and stability of film flows. In addition, a host of new issues arise due to interactions with the plasma, such as sputtering, evaporation, and behavior during disruptions [10].

Figure 7. General Design Stategies for Self-Cooled Liquid Metal Blankets

2.4. Recent Progress

2.4.1 Design concepts

Liquid metals have been adopted frequently over the past 15 years in conceptual design studies for magnetic confinement fusion reactors, dating at least as far back as UWMAK-I [18]. Table 4. summarizes some of the more recent designs using liquid metals.

Table 4. Some Recent Liquid Metal Blanket Designs

Device	Breeder/Coolant
Tokamaks	
NET	LiPb/LiPb
NET	LiPb/H_2O
OTR	LiPb/LiBiPb
BCSS	Li, LiPb
TPSS	Li/Li
HFCTR	Li/FLiBe
IBC	Li
Mirrors	
TASKA	Li/Li
TASKA-M	Li, LiPb
MARS	LiPb/LiPb
Hybrid	Li/Li
RFP's	
CRFPR	LiPb & H_2O
TITAN	Li
IBC	Li

Most early blanket designs used relatively simple flow paths. Low surface heat flux or low toroidal magnetic field make the thermomechanical design problem much easier for mirrors and RFP's. For tokamaks, design complications necessary to reduce MHD effects were proposed, but there was little analytical capability or experimental data to support the designs. Simple correlations for both pressure drop and heat transfer coefficient were used – usually based on formulas for straight ducts, or empirical corrections for simple bends. Designs involving complex manifolding and mutiple-channel configurations were either avoided or modeled in a very approximate way.

Since the early 80's, several new ideas have been studied to help alleviate the thermomechanical problems associated with liquid metals. Some of the more promising of these include:

1. Insulators
2. Flow channel inserts

3. Flow tailoring
4. Instability enhancement
5. Two-phase flow
6. LMMHD power conversion

1. Insulators

For conducting ducts, the magnitude of MHD currents in fully-developed flow is determined by the conductance of the walls, which act as series resistances in the MHD circuit. In this case, the pressure gradient is proportional to the wall conductivity and thickness as given by Eg. 1.
As discussed previously, reducing the thickness is an ineffective means to expand the design window, because the stresses become larger.

For nonconducting ducts, the current passes through Hartmann layers, and the pressure gradient is given by:

$$\nabla p = \sigma_f v B^2 \frac{1}{Ha} \qquad (5)$$

where $Ha=aB\sqrt{\sigma_f/\mu}$. Typically, $Ha\sim10^4$ and $\Phi\sim10^{-2}$, so a fully-insulated duct can have 2 orders of magnitude lower pressure drop than a conducting duct (excluding the effect of bends, manifolding, and other perturbations to the flow).

The most promising structural materials are all good conductors, so the only way to fully insulate the coolant is by the use of coatings. Insulating coatings must possess simultaneously good dielectric properties, compatibility with the liquid metal, and radiation tolerance. An evaluation of insulating coatings identified CaO, BN, and possibly AlN as the most promising materials [12]. Properties of these materials under fusion conditions are still largely unknown, and much more research will be needed before their feasibility can be assured.

2. Flow channel inserts

Insulators can be used in a laminated configuration without the need for direct contact between the insulator and the coolant. Laminated structures provide a thin cladding between the insulating medium and the coolant (see figure 8). This scheme greatly decreases the problems with insulator material behavior, since integrity of the insulator is no longer crucial. In this concept, the coolant containment and structural functions are decoupled, so that a decrease in cladding thickness will not cause increased stresses. The use of insulators as coatings as well as laminates is treated in more detail in [20,21].

Figure 8. Laminated structure for MHD pressure drop reduction

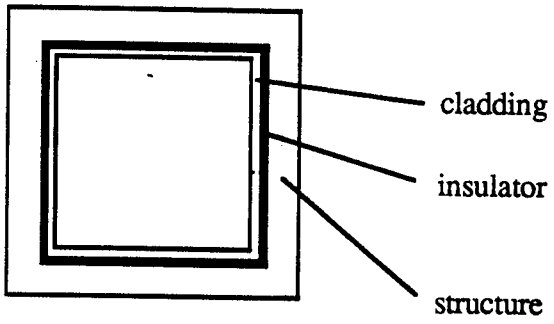

A new concept which has several engineering advantages is the flow channel insert [5]. Flow channel inserts are made by sealing a thin insulating material between two thin metal clads. This material is then formed to the shape of the channel and then inserted inside. Fabrication is relatively easy. By providing a slot or hole between the insert and the structure, the thin cladding is not subjected to large stresses due to the coolant pressure.

3. Flow tailoring

Another recent innovation is the development of methods to control MHD velocity profiles by proper design of the duct geometry, wall thickness, and wall conductivity [14]. Countering the traditional view of the magnetic field as having a universally negative impact on liquid metal blankets, so-called "flow tailoring" techniques use the magnetic field to assist in directing the flow towards regions of maximum benefit. This usually involves directing more flow close to the first wall, where the surface heat flux can cause large temperature gradients in both the structure and coolant.

Two primary forms of flow tailoring are achieved by varying either the wall conductance or the cross sectional shape. Recent experiments in a variable cross-section channel have shown good agreement between data and model predictions using the core flow approach (described below) [15]. For constant flow rate, flow tailoring normally reduces the peak wall temperatures, but increases the pressure drop due to added perturbations to the

flow. On the whole, there is a net increase in the design window.

4. Instability enhancement

It has long been known that magnetic fields suppress random turbulence in liquid metal flows [26,45]. This causes the heat transfer coefficient to degrade substantially, and also creates a fully three-dimensional temperature field in liquid meal blankets (since the thermal entry length becomes quite long). Vorticity parallel to the field is known to be much less strongly suppressed as compared to vorticity perpendicular to the field, thus leading in some cases to a two-dimensional form of turbulence .

Studies of the 2-dimensional structure of MHD turbulence at low magnetic field have been ongoing for many years [46,50]. In addition, as long ago as 1965, Hunt proposed that side layers could, in some cases, have a destabilizing effect on the flow even at very high magnetic field — contrary to the common assumption at that time [16]. An earlier work by Lehnert observed a similar phenomenon [51]. However, it has been only recently that data and analysis have indicated that instability could exist and/or be enhanced at reactor values of the magnetic field [17,18].

It is believed that perpendicular vorticity can be enhanced either through the placement of obstructions in the flow aligned with the field, or by simply exploiting the side layers which occur naturally when a duct wall is parallel to the field. Recently, linear perturbation analysis of Hunt's problem has indicated that the critical Reynolds number drops by 2 orders of magnitude as the magnetic field increases and narrow side jets form [19]. Data at high magnetic field in rectangular ducts have shown levels of fluctuating velocity as large as the average velocity [18]. This suggests that large improvements in the heat transfer coefficient may result without accompanying increases in the pressure gradient. Experiments are now being planned to further explore this effect [20].

5. Two-phase flow

An effective method to reduce the MHD pressure drop is to reduce the fluid conductivity. A two-phase mixture of liquid metal and gas is particularly attractive, since the conductivity of the gas phase is very low. This technique has been proposed using a mixture of liquid lithium and helium, operating in an annular-dispersed flow regime. Several studies of two-phase flow have been done in recent years [25,43].

Two-phase flow is very complicated, and most of the studies to date have been empirical. The two-phase mixture has less heat-carrying capacity than pure liquid; however, by reducing the MHD pressure drop, it is possible to increase the flow rate and thus enhance heat transfer. Studies have shown that there is a net advantage relative to single-phase flow when the design is optimized. However, additional issues arise, such as corrosion at high velocities and flow stability.

6. LMMHD power conversion

One of the attractive features of liquid metals is the potential for high temperature operation, leading to high thermodynamic efficiency for power conversion. To further exploit this advantage, power cycles have recently been studied using liquid metal MHD power conversion [21,52,53].

Liquid metal MHD power conversion is uniquely suited for use with liquid metals. In one possible application, a working gas is added to the liquid metal coolant after it passes through the blanket. The gas expands, driving the 2-phase mixture through an external magnet. The interaction of the magnetic field with the working fluid creates an electromotive force, which drives DC current through an external circuit. Following the MHD generator, the gas and liquid metal are separated. The liquid metal is returned to the blanket, and the gas is passed through heat exchangers to reject heat, completing the thermodynamic cycle.

2.4.2. Major experimental facilities and recent results

The major facilities for liquid metal fusion research are MHD loops and corrosion loops. Several of these are currently in operation in the U.S., Japan, Europe, and the U.S.S.R. In this section, some of the more important facilities are described, and recent results are discussed.

1. MHD facilities

For MHD fluid flow, the most important parameters which determine the features of the flow include the Hartmann number (Ha) and interaction parameter (N):

$$Ha = a\,B\sqrt{\frac{\sigma}{\mu}} \qquad N = \frac{Ha^2}{Re}$$

$$Re = \frac{\rho a v}{\mu} \qquad (6)$$

It is desirable to achieve parameters in experimental facilities which are close to those under fusion conditions. Given prototypical material properties, it is desirable to have both high magnetic field strength and large volume in order to maintain Ha and N high, as well as to provide the ability to fit relatively complex geometric elements within the magnet.

Figure 9 shows parameter ranges for several existing experiments as well as the range for typical tokamak fusion blankets. For convenience, most MHD facilities use simulant materials which are safer and/or easier to handle than Li and LiPb. The most common are Na-K and Ga-In-Sn eutectics.

Figure 9. Parameter Ranges for MHD Facilities

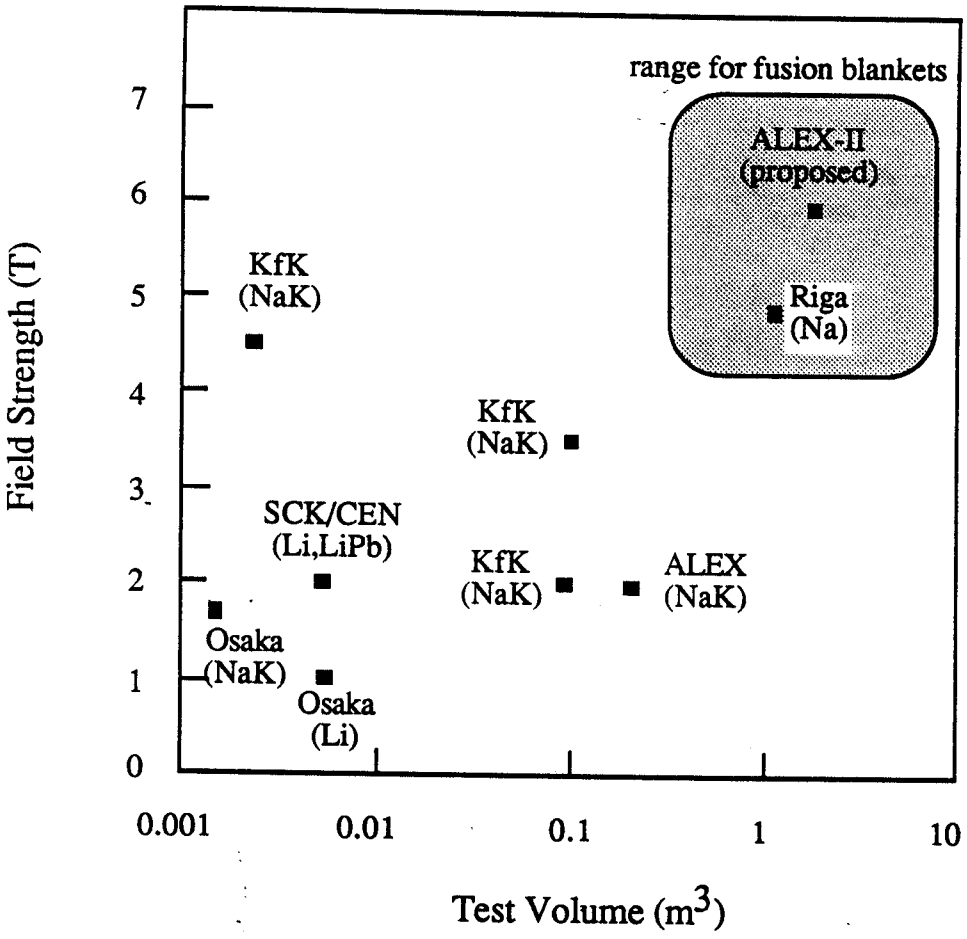

ALEX is the major MHD facility in the U.S. [22]. The facility consists of a large dipole magnet with maximum field strength of ~2 T and volume of ~0.3 m^3. The NaK loop provides a maximum flow rate of 26.5 l/s. ALEX began operating in 1985. Data has been taken for straight conducting ducts with circular and rectangular cross sections. Recently, a flow tailoring test section was tested, having a varying rectangular cross section and different conductivities on the different walls. Data includes pressures, electric potentials, and velocity profiles.

The two largest MHD facilities in Europe are: MEKKA at KfK in Germany [23], and MALICE at CEN/SCK in Belgium [24].

2.4.3. Modeling and Analysis

For reactor design purposes, the most important parameters to predict are the pressure gradient (and total pressure drop) and temperature profiles. The velocity profiles are important primarily because of their influence on temperature profiles.

Calculational techniques for pressure drop representative of the state of the art 15 years ago are given in [26]. Relatively accurate formulas were available for fully-developed flow in straight ducts. To account for bends and other three-dimensional effects, reactor design studies primarily relied on simple correlations based on experimental and analytical investigations. Detailed MHD velcocity profiles were previously available for only a limited set of geometries. Even in these cases, often the nature of analytic solutions made it very difficult to incorporate the results into a numerical heat transfer solution.

Early heat transfer calculations are summarized in [26,27]. Generally, heat transfer coefficients were determined based on simplified (such as slug flow) or assumed velocity profiles. Since most MHD flow profiles are laminarized by a strong magnetic field, entry lengths for temperature profile development are long, resulting in fully three-dimensional temperature profiles – even when the velocity profile is fully-developed.

2.4.3.1. MHD fluid flow modeling

Modeling of MHD flow several years ago was dominated primarily by analytic solutions using asymptotic techniques [28,29]. The concept of core flow and MHD boundary layers was firmly established, and a general technique for calculating velocity profiles and pressure drops for pure core flow was known [30]. The core is a region in which viscous and inertial effects are negligible, which, in most cases of fusion interest, covers the majority of the duct. In this region, the full momentum equation:

$$\frac{1}{N}(\underline{v} \cdot \nabla)\,\underline{v} = -\nabla p + \underline{J} \times \underline{B} + \frac{1}{Ha^2}\nabla^2 \underline{v} \qquad (7)$$

reduces to the simple linear equation:

$$\nabla p = \underline{J} \times \underline{B} \qquad (8)$$

Here the momentum equation has been normalized with the characteristic nondimensional MHD parameters Ha and N – the Hartmann number and interaction parameter, which measure the relative magnitude of the viscous and inertial forces as compared to the elecromagnetic body force.

MHD boundary layers form in regions where inertial and/or viscous forces are significant. The behavior of Hartmann layers and side layers has long been understood on a physical basis.

A number of simple single-duct geometries had been analyzed, including various wall conductance ratios, cross section shapes, expansions and contractions, and variable transverse field strength. Some analysis of bends and flow parallel to the mag-

netic field was performed. The number of papers in the literature covering these topics is too large to list.

Prior to the 1980's there was virtually no capabilities for accurate analysis of fusion components, which are often composed of curved pipes with bends, manifolding, and complex magnetic fields. For analysis of more complex components, a numerical solution technique was needed. First attempts at numerical modeling were performed by several researchers with limited success [31,33]. In most cases, the solutions were obtained only for very low Ha and N – in the range of 5–10. Solutions at higher parameter ranges were very difficult due to the computational problems associated with the solution of the full MHD equations.

MHD effects in liquid metal components are strongly affected by the geometry of both the magnetic field and structure, as well as the material properties and flow conditions. Table 5 lists the important factors which must be considered in developing MHD models. The number of possible design variations for self-cooled liquid metal blankets is large. However, to simplify the task of analysis, the majority of designs can be broken down into the elemental parts. The principal geometric elements of liquid-metal-cooled blankets are summarized in Table 6.

Recent attempts at numerical modeling of MHD fluid flow follow one of two major approaches:
1. core flow solutions, which assume that the magnetic field is large enough to neglect inertial and viscous effects, and 2. full solution of the MHD equations, including all terms in the Navier-Stokes equation. In addition to these, a number of analytic and approximate solutions for specific geometries have been developed recently.

Table 5. Classification of Important Parameters for MHD Fluid Flow and Pressure Drop Calculations:

magnetic field geometries	Duct geometry Wall conductance regime thin conducting ducts insulated ducts Magnetic field geometry Relationship between the duct and Flow regime (Ha, N, Re_m, etc.)

Table 6. Geometric Elements of Blankets and High Heat Flux Components

contouring)	straight uniform ducts varying cross-section smoothly-varying cross-section (e.g., flow tailoring or toroidal
manifold)	abruptly-varying cross-section (e.g., an orifice or section of a
	bends smooth bends a. no parallel flow b. parallel flow abrupt bends a. no parallel flow b. parallel flow internal flow redirection (e.g., helical vanes) multiple-channel ducts and manifolds wall conductance tailoring

1. Core flow approach

Different numerical methods have been developed to solve the core flow equations. While it is straightforward to solve directly the three-dimensional system of 8 equations in 8 unknowns, it is computationally much more efficient to reduce the equations using various techniques. It is possible, using the unique feaures of the core equations, to reduce the problem to a two-dimensional problem with 4 equations and 4 unknows. The complete three-dimensional flow field can be represented in terms of these four two-dimensional functions. The two major

techniques for solving the reduced core equations are: direct integration by Kulikovskii's method and the iterative solution method.

Applications of the direct method are described in [30,34,35]. A variety of geometries and wall conductance ratios have been analyzed, including circular and rectangular ducts, conducting and insulating walls, and varying transverse and longitudinal fields. At this time, analysis using the direct solution has not been reported for multiple-channel configurations.

The iterative method was developed to solve complex geometries, in which the direct method may be difficult to formulate. The iterative method solves the same set of equations as the direct method, but does so in separate steps. The electrical and fluid parts of the equations are solved separately, resulting in a much simpler set of equations.

The first application of the iterative method examined a multiple channel bend with the flow turning from perpendicular to parallel to the field direction [1]. This first model was simplified in such a way as to yield only approximatie solutions. Subsequently, the method was improved to exactly solve the core equations, and it has been applied to a variety of problems, including varying cross section, varying field, bends, and multiple-duct configurations [36,49].

2. Full Solution

The Full Solution is a general method for MHD flows in the sense that no fundamental approximations are made to the system of equations. All of the terms are retained in the Navier-Stokes equation, and the equations are treated in a fully-three-dimensional way. The Full Solution has advantages over the core flow approach in certain situations, including: 1. parameter ranges in which inertia and viscosity cannot be neglected, 2. certain geometries where inertial effects can be significant even at high Ha and N (for example, abrupt changes in geometry or flow situations which have a large parallel component of magnetic field), 3. situations where heat and mass transfer strongly depend on the detailed characteristics of boundary layers, 4. transient problems where the flow behaviors in boundary layers and in the core are different. The Full Solution approach has a wider potential range of applicability compared with other approaches. However, numerical difficulties have limited the ability to solve problems in which the interaction parameter (N) and Hartmann number (M) are large.

Before 1984, the accomplishments of this solution approach were very limited. The effect of changing the orientation of the applied magnetic field and wall conductivity on the fully developed velocity profile in a duct had been examined. Also,

developing flows in a two-dimensional channel (with N = 3.5) and fully developed flow in a duct with an arbitrary cross section (with M ~ 5) had been studied.

Since then, the capability for numerical prediction of MHD flows has been enhanced greatly. The main accomplishments have been an extension of the parameter ranges which can now be investigated, and expansion of the dimensionality from two- to three-dimensional problems.

In 1986, Ramos and Winowich [63] obtained a velocity field of steady, two-dimensional MHD flow in a channel with N=10, M=100. In 1987, Abdou et al. [54] investigated a two-dimensional MHD flow in a channel. They studied two cases: 1) magnetic field parallel to the main flow direction, and 2) magnetic field perpendicular to the flow direction. For the first case, they obtained the profiles of the velocity and temperature in the region of developing flow. For the second case, fully developed velocity profiles at different combinations of M and Re (orders of both up to 100) were obtained and the effect of the magnetic field on heat transfer in the entry length region was studied.

It has been understood that realistic MHD flows include three-dimensional effects. Recent efforts that focused on the prediction of three-dimensional MHD flows have been greatly aided by the development of fast-running computers with large memory capacity and the use of sophisticated numerical methods. Aitov [44] calculated a flow in a channel with sudden expansion with N order of up to 100 under a uniform magnetic field. The duct walls are all electrically insulating. In this research he found out that inertial effect cannot be neglected in a flow where M is much larger than N, even under a strong magnetic field. In 1989, Sterl solved MHD flows in a rectangular duct with a nonuniform magnetic field with M=100 using the thin wall approximation [38]. The solution procedure employed the use of Fast Poisson Solver with uniform grid. In 1989, Kim and Abdou [37] predicted MHD flows in a rectangular channel with/without sudden expansion under a uniform/nonuniform magnetic field. Flow fields were calculated for arbitrary wall conductivities with M=N=100. In this work, the sizes of the terms in the equation of motion were estimated and it was shown that the inertial term cannot be neglected in a sudden expansion. Also, they studied the effect of the direction of magnetic field on the flow field.

Heat transfer characteristics can be obtained from the predicted velocity field. In 1988, Kim and Abdou calculated velocity and heat transfer for a three-dimensional MHD flow in a straight rectangular channel with nonuniform magnetic field for M=100, N=100, Pe=150 [48]. The duct walls are thermally and electrically conducting.

The recent development of the solution method enables one to solve flow and temperature fields in a three-dimensional geometry which can be configured by Cartesian coordinates with an arbitrary combination of the electrical conductivities of duct walls under an arbitrarily applied magnetic field.

As mentioned in brief earlier, numerical difficulties are usually met when the interaction parameter (N) and Hartmann number (M) are larger. These difficulties are associated with possibly large discretization error and slow computation with the use of small relaxation parameters. Therefore, the main efforts should be focused on the improvement of numerical scheme that would provide accurate results with high speed of computation even with high interaction parameter and Hartmann number. For the practical application of the liquid metal MHD flows, prediction of the flow fields in a realistic geometry should be enabled. For this purpose, MHD flows in a body-fitted coordinate should be investigated. Also, transient behavior of MHD flows should also be studied to fully understand the flow characteristics in the application.

3. Analytic solutions

In addition to the numerical solutions described above, analytic solutions for individual geometries have been ongoing over the past years. Analytic solutions are now available for conducting and insulating ducts with varying cross section, varying transverse magnetic field, and single-channel bends.

4. Approximate methods

A small amount of analysis has been done using "approximate" methods to estimate pressure drop and in some cases velocity profiles [1]. These methods usually make apriori assumptions about either the shape of the velocity profiles or direction of the streamlines. For example, a possible approach is to assume slug flow conditions. By assuming a known velocity field, it is much easier to compute the electric fields and currents, and thus the pressure field. This approach allows solutions in very complex structures, since the MHD equations are not solved directly.

2.4.3.2 Heat Transfer

Strong magnetic fields are known to laminarize MHD fluid flow [26,45]. In this case, the energy equation is relatively straightforward to solve. However, since the velocity profile is generally three-dimensional, analytic solutions for heat transfer are extremely limited. Numerical solutions for laminar flow conditions have been obtained primarily in straight ducts [39,40].

One of the important issues remaining for laminar MHD heat transfer is the effect of MHD boundary layers. For example, it was shown in [85] that the peak wall temperatures are strongly dependent on the velocity profile in side layers. Small changes in the direction of the magnetic field can lead to changes in the width, shape, and peak velocity in side layers, leading to significant changes in the wall temperatures.

Another important issue for heat transfer is the possible presence of nonlaminar flow at high magnetic fields. Experiments have been performed in Israel and the Soviet Union [17] at relatively low magnetic field strength, but the results suggest that two-dimensional turbulence might be enhanced even at reactor values of the magnetic field strength. Modeling of nonlaminar flow is very difficult, and little work has been done to help predict the effects on heat transfer.

TABLE 7

TABLE OF MAIN SOLID BREEDER BLANKET MATERIAL AND CONFIGURATION OPTIONS

MATERIALS

Solid breeder	Li_2O, Li_4SiO_4, $LiAlO_2$ Li_2ZrO_3
Multiplier	Be or possibly nonewith Li_2O
Structure	Ferritic or Austenitic
Coolant	Helium or Water
Purge	Helium + $\%H_2$

MATERIAL FORM

Solid breeder and Multiplier	Sphere-pac or sintered block
Configuration	Breeder-in-tube, Breeder-outside tube, Layers

3. SOLID BREEDER BLANKETS

3.1 INTRODUCTION

Interest within the fusion community in solid lithium compounds as tritium breeders in power reactor blankets has grown considerably since the late 1970's. The solid breeders offer potentially attractive alternatives to liquid breeders. They avoid MHD problems, and in general have minimal or no chemical reactivity with candidate blanket coolants and other materials in reactor nuclear systems. However, there are issues which need to be addressed such as the potential effects of radiation on tritium release characteristics,temperature control of solid breeders, and the need for a neutron multiplier.

3.2 DESIGN OPTIONS

The main solid breeder material and configuration options for a fusion reactor blanket are summarized in Table 7. The options apply for commercial fusion power reactor or for an experimental reactor which would typically operate at a much lower power density and which would require tritium breeding but not necessarily power production. The four breeding materials shown will require the use of a neutron multiplier (Be) to achieve adequate tritium breeding, with the possible exception of Li_2O which has the highest Li atom density. Li_2O is also attractive based on tritium release followed by Li_2ZrO_3 and Li_4SiO_4. Li_2O is also favored based on low activation and so is Li_4SiO_4. However, Li_2O in particular is hygroscopic and exhibits poor chemical stability. $LiAlO_2$ has the poorest tritium breeding and tritium release characteristics but is the most chemically stable which warrants its inclusion as a solid breeder of interest [54,57].

Be is probably the only multiplier of interest in conjunction with solid breeders, mainly because Pb, the primary alternative, suffers from stringent maximum temperature limitations based on its low melting point and corrosion characteristics, and from a relatively high threshold for the (n,2n) reaction.

The material form options for both the solid breeder and Be are sintered block and sphere-pac. For Be, the sintered block provides benefits of high thermal conductivity and possible design simplicity. Issues include effects of thermal expansion, thermal stresses and prediction of thermal resistance at clad interfaces. The sphere-pac form which is basically a packed particle bed is of particular interest for Be for cases where temperature control is required (e.g. to accommodate power variation) since the particle bed thermal conductivity could be controlled through purge gas adjustments. However, the effective thermal conductivity of a Be packed bed is significantly lower than that of a sintered block. For solid breeders, the attractiveness of sphere-pac rests mainly on its potential for uniform and predictable behavior under operating conditions as opposed to a sintered block which might crack or fragment due to high thermal stresses and whose interface conductance might vary considerably.

The choice of structural material will depend on the operating conditions of the reactor. Cyclic operation, for example, could favor austenitic if the temperature is pulsed below and above the low ductile-to-brittle transition temperature of ferritics. However, ferritic steels can operate at higher temperatures and result in lower long-term activation compared to austinitic steels. The vanadium alloys generally favored for liquid breeders are not considered with solid breeders because of incompatibility with water coolants and with impurities e.g. oxygen, normally present in helium coolants.

He and H_2O have been used extensively in fission reactors and their problems are considered to be well understood. They are the coolant choices here. Neither is influenced by the magnetic field. Water has excellent heat transfer characteristics and enjoys a well-developed technology for use in power conversion systems. Its primary disadvantages are lower thermal energy conversion efficiency and the high pressures required for containment in a power reactor. The primary advantage of helium is that it can be operated at high temperatures without an absolute need for very high pressures and it is chemically inert. Its principal disadvantage relates to its low volumetric heat capacity and radiation streaming [72]

A purge gas, normally low pressure helium, flows through the solid breeder and is solely used for in-situ removal of the tritium generated there so that it can be transported out of the reactor to be processed and used as fuel for the fusion reaction, thereby closing the fuel cycle. The purge flow rate is low. Helium is the preferred purge gas since it is inert and tritium removal from helium has been demonstrated in several experiments. The addition of a small volume fraction of H_2 in the purge (<1%) facilitates the tritium recovery through isotope swamping.

Of the three configuration options listed in Table 7, the breeder-outside-tube (BOT) option is particularly well suited for the power reactor water coolant case. The high pressure coolant flows in tubes which can accommodate the pressure with the minimum amount of structure and could be double walled for added reliability. The breeder is located outside the tubes and the configuration results in minimum volume-fractions of neutron-absorbing steel and adequate volume fraction for tritium breeder as compared to the other configurations. Fig. 10 shows an example of such a blanket [42] which is modular (i.e., the blanket is made up of a number of adjacent modules) with a semi-cylindrical actively cooled first wall. The interior of the blanket is all breeding zone. In this case, the first 20 cm of the breeding area contains a mixture of 90/10 Be and $LiAlO_2$ breeder to provide the neutron multiplication for enhancing tritium breeding. The remaining 32 cm is all $LiAlO_2$. Both $LiAlO_2$ and Be are in sphere-pac form with packing fractions of 80%. The sphere-pac form provides the possibility of adjusting the effective thermal conductivity through control of the helium purge pressure so as to effectively keep the solid breeder temperature at the desired operating level for adequate tritium release. The blanket is cooled with pressurized water flowing in double-wall coolant tubes with a maximum pressure of 15 MPa, and inlet and outlet temperatures of 280°C and 320°C respectively. The tubes are spaced according to the blanket power density which decreases exponentially with distance away from the plasma.

Figure 11 shows an example of a helium-cooled layered solid breeder blanket with the solid breeder contained in plate-type geometry [42]. It is a pressurized module design containing the 5 MPa helium. To provide adequate tritium breeding, beryllium rods are placed in front of the solid breeder plates for neutron multiplication. The plate geometry maximizes the blanket breeder volume fraction. A separate helium purge passes through the breeder plates for tritium extraction. Coolant helium flows through the module side inlet channels toward the plasma, cools the first wall and turns at the apex of the module. It then flows radially upward to cool the beryllium rods and breeder plates.

The two blanket examples above are for power reactors. For a fusion experimental reactor, such as the International Thermonuclear Experimental Reactor (ITER), the blanket requirements are different. Tritium still needs to be produced but power generation is not required. Thus, safety and reliability considerations point to a tritium-producing blanket with moderate coolant temperature and pressure. A worthwhile objective is to try to decouple the breeder operating temperature which should be high (typically 400 - 800°C) for tritium release from

the coolant temperature. which should be low for reliability and safety. A U.S. design for such a blanket is illustrated in Fig. 12 [58],59. It uses a layered configuration whereby the temperature difference between the solid breeder and water coolant is provided by a Be layer. The two layers of Li_2O breeder have minimum and maximum temperatures of 395°C and 487°C while the water pressure and water inlet and outlet temperatures are 0.6 MPa, and 20°C and 40°C respectively. The layered approach in this context is believed to have advantages of simplicity and relative economy. The Be layer can either be a thick sintered block layer or a thinner sphere-pac region. The advantages of the sintered block form here are its high thermal conductivity and relative design simplicity, while the sphere-pac form offers advantages of potential breeder temperature control.

A Japanese blanket design for ITER proposes the use of a 75/25 homogeneous mixture of Be and Li_2O pebbles of 1 mm diameter with maximum packing fraction of 60%[59]. The configuration is shown in Fig. 13 and has the 1 MPa water coolant flowing in tubes with inlet and outlet temperatures of 50°C and 100°C respectively. The proposed breeder temperature control is a pressure-controlled helium gas gap surrounding the coolant tubes. The breeder region is purged by helium. This type of Be/solid breeder homogeneous mixture is believed to provide for maximum tritium breeding. However, the compatibility of Be and solid breeders, particularly in the radiation environment, still needs to be assessed.

Fig. 14 shows cross-sections of a European concept for a solid breeder blanket for an ITER-type device such as net [5]. The proposed concept is modular and consists of radial layers of Be and solid breeder. The coolant is 6MPa helium with inlet and outlet temperatures of 200°C and 450°C which are close to power reactor conditions. Thus, whereas the two previous concepts are for the basic blanket and they focus on moderate temperature and pressure for reliability and safety, the goal here is to operate a blanket test module at its maximum possible performance for the given conditions of the experimental reactor. Two independent coolant systems are used for safety reasons. In the breeding region the coolant flows through tubes within the Be layers while the helium purge flows through the breeder plate region which contains sphere-pac Li_4SiO_4. The Be and Li_4SiO_4 layers have thicknesses of 21mm and 6 mm respectively resulting in reasonable tritium breeding. Similar blankets with a BIT configuration are described in References [61,62].

The next section will cover in more detail thermomechanics issues relevant to the different solid breeder configurations.

3.3 SOLIC BREEDER ISSUES

Several major solid breeder issues and problems are broadly associated with the thermomechanical area. They include:
1. Breeder/multiplier tritium inventory , recovery and containment
2. Breeder/multiplier/structure mechanical interactions;
3. Operation under off normal and accident conditions;
4. Structure mechanical behavior; failure modes and reliability;
5. Corrosion and mass transfer.

I should be noted that attaining adequate tritium breeding ratio is a critical issue [9] for solidbreeder blandets, which strongly influences the thermomechanical design issues. These issues are discussed below.

3.3.1 Breeder/Multiplier Tritium Inventory, Recovery and Containment

Tritium recovery and control require understanding the retention and transport of tritium within the breeder and multiplier. The objective is to minimize the inventory of radioactive tritium in the solid breeder and multiplier which could be liberated under accident conditions. Typically, as shown in Fig. 15, the tritium atom bred in the solid breeder diffuses through the solid breeder grain, then through the grain boundary to the bulk/pore interface where tritium adsorption from the bulk to the pore surface occurs. Tritium then desorbs to the pores in molecular form, diffuses along interconnected porosity, and is finally convected by the helium purge to the processing systems where it is recovered. All the above transport mechanisms are strongly influenced by the operating temperature range. For example, the characteristic time for tritium diffusion in $LiAlO_2$ can increase by an order of magnitude under a temperature decrease of 100 K, as shown in Fig. 16. In addition, characteristics of the purge such as its composition and flow rate also play an important role. Tritium containment also falls under this broad category ; the main concern is the permeation of tritium from the purge to the main coolant.

The combination of an allowable temperature window set by tritium release considerations with a low thermal conductivity and a high volumetric heat generation close to the first wall results in strict design constraints. It also affects the degree of operating flexibility of the blanket. Table 8 shows the thermal conductivity of and typical temperature limits imposed on the four major solid breeders of interest. The lower temperature limit is generally dictated by the need to have fast enough tritium transport processes, such as intergranular diffusion, to prevent high tritium inventories. The higher temperature limit is usually based on the occurrence of sintering which would close the solid

breeder pores, thereby hampering tritium release. The higher temperature could also be limited by mass transfer considerations; e.g. mass transfer of Li OT in Li_2O.

Solid Breeder	Thermal Conductivity at 1000 K (W/m - K)		T_{max} (K)	T_{min} (K)
	Unirradiated	1MW-yr/m^2 irradiation		
Li_2O	3.8	2.5	1073	673
Li_2ZrO_3	1.8	1.3	1242	573
Li_4SiO_4	2.0	1.5	1000	623
$LiAlO_2$	2.5	2.0	1242	673

Table 8 Examples of solid breeder thermal conductivity and lower and upper operating temperature limits [54,63]

The imposed design constraints can be illustrated by using Li_2O as an example and assuming a typical heat generation of 50 W/cm^3 in the first solid breeder region. Even when making full use of the Li_2O temperature window, the allowable solid breeder first region thickness is limited to only about 9 mm. This thickness would be reduced even further to account for uncertainties and/or variation in the power level. These uncertainties range from basic properties such as the thermal conductivity of irradiated materials to complex integrated effects such as the thermal resistance of the interface between the structure and solid breeders in a fusion environment. These constraints on the solid breeder region thickness result in multi-layer designs or multi-row designs for the BIT or BOT approaches. Since each solid breeder region must be cladded, the volume fraction of structure increases with the number of solid breeder regions thereby reducing the tritium breeding performance. Thus, one of the challenges of designing a solid breeder blanket is to optimize the design within the given constraints so that the resulting volume fraction and location of solid breeder, multiplier and structure yield the maximum possible tritium breeding to amply cover uncertainties in the breeding predictions [64].

The purge flow characteristics can affect the tritium release behavior. For example, addition of small volume percentage of oxygen tends to increase the tritium inventory. Addition of up to about 1% by volume of hydrogen has the opposite effect and is thus used to boost the tritium release. For example, Fig. 17 shows the effect of increasing the hydrogen content in the purge from He = 0.01%H_2 to He = 0.1% H_2 on the tritium release for a Li_2ZrO_3 sample in the MOZART experiment [65]. The tritium release is increased tremendously before returning to the steady state level. This can be explained by the hydrogen swamping the adsorption sites on the solid breeder and thus releasing the tritium originally covering the sites. Another consideration that seems to be in conflict with tritium release is tritium permeation from the breeder to the coolant. Adding hydrogen to the purge gas can increase tritium permeation while adding oxygen can reduce it.

Flow rate is another purge characteristic which can influence the tritium release since the partial pressure of tritium in the purge is directly proportional to its flow rate for a given tritium generation rate. The partial pressure of tritium in time influences tritium adsorption and dissolution in the solid breeder. Even though the purge flow rate is small since tritium removal is its only function, the flow inside the breeder area for the purge is also small for maximization of solid breeder volume fraction inside the clad. The resulting pressure drop for the purge can thus be high enough to constrain the flow rate.

For example, Fig. 18 shows the purge pressure drop along a sphere-pac solid breeder channel as a function of the porosity for different Reynolds numbers and sphere diameter to channel width ratios [66]. The corresponding pumping power for a typical total blanket flow rate of $3m^3/s$ is also shown and can be seen to be reasonably low for sphere diameter-to-channel width ratios greater than 0.1 and porosities greater than 0.2. For porosities of about 0.15 - 0.2, as proposed in past designs [42], the pressure drop is a binding constraint, being about 1 MPa for a Re of 10. Typically the purge pressure is kept lower than the coolant pressure to minimize tritium contamination of the coolant in case of leaks. For a commercial helium-cooled reactor, the coolant pressure is about 5-6 MPa[42] whereas for an ITER-like reactor the coolant pressure is closer to 1 MPa[58]. From Fig. 18, increasing the Re from 10 to 100 would increase the pressure drop by one order of magnitude, which is unacceptable.

Finally, tritium containment concerns relate mainly to uncertainties in permeation affecting safety (tritium loss rate to the environment), waste management (tritium imbedded in blanket structure), and maintenance (tritium levels in the primary system and reactor hall). Permeation barriers, such as an oxide layer, substantially help in reducing permeation. Imposed limits on permeation in effect are limits on the tritium partial pressure in the purge and, thus, on the purge flow rate for a given generation rate. Figure 19 shows the limiting HT partial pressure for a $LiAlO_2/H_2O$/HT9/Be blanket [42] assuming 100 wppm H_2 in the purge as a function of the permeation limits for a possible range of barrier factors (represented by IF). It is clear that barrier factors can considerably alleviate the constraint on the purge mass flow rate.

These are the types of considerations which are part of trade-offs, in this case effectively between purge flow area and tritium partial pressure, exerting opposite constraints on the purge flow rate, for solid breeder blanket design.

3.3.2 Breeder/Multiplier/Structure Mechanical Interactions

The interface between the breeder/multiplier and the surrounding blanket, normally through a metallic cladding, can be an area where stress and heat transfer limits occur. Uncertainties include the mutual loads and responses imposed by the elements on each other. These can be caused, for example, by swelling, (which is of particular concern for Li_2O and Be as shown in Figs. 20 and 21.

Changes in the effective gap thermal resistance at the breeder and clad interface affects the operating temperature range of the breeder for a given coolant temperature since it changes the temperature rise between the coolant and breeder. In this case, the separation distance between the solid breeder and clad boundaries is a key factor that can change during operation due to a number of processes including: (1) differential thermal expansion between solid breeder and structural materials, (2) solid breeder cracking and cracked fragment relocation,
(3) solid breeder densification due to thermal/radiation-enhanced sintering,
(4) solid breeder thermal and radiation-enhanced creep, (5) solid breeder radiation-induced swelling, and (6) time-dependent deformation, such as creep and swelling of the structural materials.

The effect of the separation between breeder and clad and of the temperature on the gap conductance is illustrated in Fig. 22 for the upper bound case when the separation is much larger than the temperature jump distance [41]. The effect of changes in the separation on the gap conductance is more marked at high temperatures and correspondingly, the effect of an increase in temperature on the gap conductance is substantially higher for the smallest separation (1mm in this case). The temperature effect on the gap conductance here is basically due to the helium thermal conductivity increasing with temperature. Note that for comparable geometries, the effect of a change in the separation on the overall region temperature drop will be much more severe for a Be/clad interface than for a solid breeder/clad interface since the thermal conductivity of Be is higher than that of a solid breeder by a factor of 60 or more.

This particular thermomechanics area is an important consideration in the choice of material form based on analyses in references such as [54,42,67,68]. The sintered block form offers high conductivity (in particular for Be) and potential design simplification but suffers from gap conductance uncertainties, thermal stress and cracking problems. The sphere-pace resolves the cracking problem and is not as

vulnerable to changes in gap conducture. However, its thermal conductivity is lower than that of the sintered block (substantially lower in the case of Be).

Information required to reduce uncertainties in this area and to help in the choice of the material form include: (i) swelling data for breeder ceramics and Be as a function of temperature, microstructure and reactor-like fluence, and (ii) effective thermal conductivity data including the interface conductance for Be and breeder ceramics (for both sintered block and sphere pac forms) as a function of temperature, porosity and reactor-like fluence.

3.3.4 Off-Normal and Accident Conditions

Among the off-normal conditions of concern are those operation changes that can affect the solid breeder operating temperature range causing it to violate either the low or high temperature limits. For example, both power reactors and experimental reactors will be required to operate at power levels different from their design points. Operation at power levels as low as about 5% may be necessary for extended periods for such purposes as startup and low-power operation during the licensing period, or checkout of newly-installed components such as replacement steam generators. In addition, uncertainties in the thermal behavior of the blanket such as gap conductance might result in the solid breeder operating range being lower or higher than the design point, in particular for an experimental reactor blanket. Clearly, a blanket that can be designed to handle power variation and related uncertainties would provide substantial operation flexibility and be particularly attractive.

An example of a design decoupling the solid breeder temperature from the coolant temperature is shown in fig. 13. In this design, a thin helium gap provides the required thermal resistance. Because of the low conductivity of helium, this gap is small, about 1mm, and can possibly be used to control the solid breeder temperature through adjustment of the gap gas pressure (or even composition). However, such a small gap is vulnerable to geometry changes during operation. Another means of decoupling the solid breeder and coolant temperatures is shown in the design of Fig. 12, where a large Be region provides for the temperature drop between the hot solid breeder and cold coolant. In any case, a certain amount of power increase can be accommodated by allowing the solid breeder operating temperature range to rise within the allowable temperature window. For the design of Fig.12, active control over the Be thermal conductivity would substantially increase the allowable power variation for the blanket. For example, Figure 23 shows the allowable power increase for the blanket of Fig. 12 as a function of the uncertainty in the Be region thermal conductivity for different controllability levels. The initial Li_2O operating temperature range is 400°C - 500°C and two cases of maximum allowable Li_2O temperature are shown: (1)800°C on the left vertical axis and 1000°C on the right vertical axis. The dashed line corresponds to a sintered block Be region and includes the decrease in Be thermal conductivity with rising temperature. For an assumed uncertainty of 20% in the Be thermal conductivity and a maximum allowable Li_2O temperature of 800°C, the allowable power increase in increased from about 15% to 60% going from a sintered block case to a mere 30% controllability case. This active control could be provided by the Be purge pressure, flow rate or composition changes if the Be sphere-pace form is used. Few experimental

data are available for packed bed effective thermal conductivity as a function of pressure for Be-like solid thermal conductivity and helium. However, Fig. 24[69] gives an indication of the effect of pressure of single-size packed bed with 40% porosity for Zr and N_2 whose ratio of conductivity is of the same order as Be and He. The effective packed bed thermal conductivity increases by about 80% when the pressure is increased from 0.1 atm to 1 atm.

There are of course other variables that need to be taken into account such as the effect of surface characteristics, lower porosity and multi-size packing. These need to be addressed experimentally but the indications from existing data and models are encouraging in that use of sphere-pace Be could provide substantial design flexibility in enabling power variation accommodation by packed bed thermal conductivity adjustment through purge gas control.

Ideally, a blanket should be designed so as to be able to passively accommodate accident conditions since it is difficult to design an emergency cooling system. Of the two commonly considered accident scenarios, loss-of-flow-accident (LOFA) and loss-of-coolant=accident (LOCA), LOCA is most severe. The safety objective is to prevent the afterheat causing volatization of activation products. The economic objective is even more binding since it is to protect loss of investment by insuring that the material (solid breeder, structure and multiplier) temperatures do not exceed the limits beyond which the materials could operate and would then have to be replaced.

Reference [70] discusses thermal limits for passive safety of fusion reactions for four different blankets, including a Li_2O/He/HT-9 blanket. The focus is on establishment of limits for first wall loads to achieve passive protection of the plant as well as public safety. Fig. 25 shows an example temperature history following a LOCA in first wall and shield of the Li_2O blanket for 5MW/m^2. In this case the analysis recommends a limit of 3-6MW/m^2 for the neutron wall loading based on acute structural failure considerations.

Another example of LOCA analysis, this time for a helium-cooled solid breeder blanket proposed for ITER[71], is discussed in Ref [73]. The results indicate that use of the helium purge can greatly help to accommodate a main flow LOCA. Fig. 26 illustrates this point by showing the first wall temperature history following a main flow LOCA for different purge velocities. Use of the purge, though, is an active measure and the ultimate objective is still to design a blanket which can passively accommodate LOCA for all flows.

3.3.5 Structure Mechanical Behavior, Failure Modes and Reliability

The major concerns in this category of issues can be divided into three areas [74]: structure mechanical response, thermal power transient response, and electromagnetic response. The structural mechanical response to the environmental conditions includes the mechanical behavior of the various structural elements during blanket operation. The major material properties which lead to loading within the structure are differential thermal expansion and the differential dimensional stability of the material at various locations throughout the blanket. These phenomena lead to loading of the structure which is relieved by creep or crack growth. These responses are then responsible for deformation of the structure which may cause operational or maintenance problems, or may lead to failure of the structure. The thermal/power transient response of the structure must also be understood so that potential failures due to this response can be minimized through appropriate design. Normal transients associated with the periodic cycling of the plasma burn can be expected whether or not the fusion device is run in a cyclic or steady-state mode. Off-normal power transients associated with disruptions for example can also be envisioned. These phenomena can lead to failure of the structure and must be adequately explored. : finally, electromagnetic forces can also lead to loading of the structure. This loading can be either steady state or transient in nature. Of particular concern are the transients associated with plasma disruptions. These can lead to large instantaneous loads on the structure, and the magnitude of these loads must be understood.

In order to effectively design blanket components with adequate structural lifetimes, it is necessary to develop understanding of these phenomena in complex geometries and over applicable environments. Perhaps the largest effort for this issue will be the development of computer models which can be used to assess blanket designs. The modelling needs include relevant material properties correlations and the extension of fracture mechanics analysis to relevant geometries. Such models could then be used to develop design criteria for the structure.

Parameters affecting structural mechanical behavior include both environmental parameter ranges and design related factors. The important environmental parameters are the maximum temperature and associated temperature gradient, and the peak fluence and associated flux gradient. The temperature gradient is the driving mechanism in the differential expansion. Both the temperature and flux gradients are responsible for the differential swelling if the material swells during its anticipated lifetime. The variation of these environmental parameters (particularly temperature and magnetic field) with time are also important when considering transient response. Examples of environmental ranges for present solid breeder blanket designs are given in the BCSS report [42]. The major design related

factors include both geometry and the joint configurations. The overall geometry leads to possible regions of stress concentrations within the structure which become potential failure sites. The joining of materials within the structure such as weldments will probably be required due to the complexity of the blanket designs. These also represent regions of dissimilar response or stress points whose responses are unknown and difficult to model.

Reliability is an important consideration but can only be thoroughly characterized through integrated experiments under conditions as prototypical as possible. Determination of mean-time-between-failures and mean-time-to-replace for the different components becomes important to evaluate the overall effect on the fusion reactor availability. More details can be found in references [1]

3.3.6 Corrosion and Mass Transfer

The material interaction issues may be divided into interface (corrosion) and bulk (mass transfer) processes [74]. These interactions and their uncertainties are briefly discussed below.

Coolant/Structure: For water or helium coolants and stainless steel structure, corrosion is acceptable but not negligible [75]. Concerns include identifying and achieving optimum coolant chemistry, corrosion product deposition and activity levels, and stress corrosion cracking[76]. Significant discrepancies in corrosion rates exist between laboratory experiments and operating values. The optimal coolant chemistry for fusion will be different because of the different operating conditions (higher energy neutrons, neutron sputtering, magnetic fields, structural alloys). However, while further development will certainly be required for commercial reactors, it does not pose feasibility concerns.

The possibility of magnetic field effects on corrosion was considered in STARFIRE[76]. Possible mechanisms were identified, but none appeared to be a major concern for steel/water systems.

Structure/Breeder: Several experiments have investigated the reactions between structural alloys (steels, transition metals) and solid breeders (Li_2O and ternary oxides) [77-80]. Early tests indicated severe corrosion by Li_2O within short periods of time (100 hrs). Subsequent experiments identified the importance of LiOH and have led to breeder operating limits in order to prevent LiOH formation near the cladding. Under these conditions, the reactions are fairly limited with 10mm scales forming over 1000 hrs, and a decreasing reaction rate. Very little reaction has been observed between the ternary oxides and steel (HT-9, 316SS) in sealed tube experiments.

Uncertainties include the effects of the burnup-induced stoichiometry changes, purge composition, and the corrosion

rate at end-of-life (> 20,000 hrs). Although not apparently life-limiting, understanding the extent and kinetics of the reactions defines temperature and possibly purge composition limits, and supports efforts to understand the influence of the clad surface on breeder oxygen activity and on tritium permeation through the clad.

Multiplier/Structure: Beryllium, the preferred multiplier, can react with steel to form a hard surface coating. It has an affinity for nickel, so NiBe is the most common compound with high nickel steels ($FeBe_2$ and BeC are also formed). Overall, however, the interaction with stainless steels would be small at the structural temperatures [77].

Multiplier/Breeder: some blanket designs propose a direct mixing of beryllium multiplier and solid breeder in order to enhance neutronics and tritium recovery, and simplify the thermomechanical design. However, there are thermodynamic concerns because of the affinity of Be for oxygen. The extent and consequences of this mixing will depend on the source of oxygen (whether the oxygen activity is maintained by the "system" or the breeder) and on the reaction kinetics. It is possible that the reaction rate may be acceptably slow after an initial BeO surface layer has formed. A BeO/breeder combination might be chemically acceptable if no further mixed oxides form (e.g., $BeAl_6O_{10}$), or at least do not degrade the behavior. The development of a phase diagram for the breeder/beryllium system is needed.

Multiplier/Coolant: Beryllium is reasonably compatible with many blanket coolants, and is in direct contact with the coolant in several designs [42]. Significant reaction with oxygen occurs over 600-800°C, after which the reaction increases rapidly until excessive embrittlement and possibly burning occurs. The behavior with nitrogen is similar but slower [76]. consequently, beryllium appears compatible with reactor-grade helium up to about 700°C, with a protective oxide layer forming[28]. High purity beryllium is compatible with low-temperature high-purity water, but corrosion occurs if the water is slightly ionized or if the beryllium is commercial-grade purity. There are no conclusive data with respect to high temperature water. Porous beryllium has a higher corrosion rate due to the increased surface area [76,81].

Coolant/Breeder: Contact with helium coolant (either directly or through leaks) does not raise significant compatibility issues for present lithium-based oxide breeder materials which are anticipated to operate with helium purge streams in many designs [57]. Contact with water can lead to formation of corrosive LiOH in Li_2O and must be avoided.

Coolant Mass Transfer: The deposition of corrosion products within the coolant stream may influence local heat transfer and flow (e.g., around spacers or other channel

discontinuities) and radioactivity levels (e.g., around valves). Present reactor experience provides design guidelines for minimizing these effects. It also appears than magnetic corrosion product particles will not be significantly restrained relative to the coolant flow [76].

Breeder Mass Transfer: Experience with fission reactor fuels suggests that 10^{-7} MPa is a critical value for the onset of appreciable vapor phase transport in a static atmosphere. Thermodynamic calculations for the Li_2O, $LiAlO_2$ and Li_4SiO_4 systems indicate significant LiOT and Li vapor pressure at higher temperatures (1000°C) and even at 600°C for Li_2O [82]. The transport of material within the breeder can lead to restructuring, grain growth and pore closure, which could significantly impact tritium recovery and breeder thermomechanical properties.

The loss of breeder material through removal of vapor is probably most significant for
Li 2O. Measured weight loss of Li_2O in flowing He at 550°C was 12%/yr with 93 ppm H_2O in the helium, 3.8%/yr with 1ppm H_2O, and 3.2%/yr in 1 ppm H_2O and 1ppm H_2 [77]. This is 2-3 orders of magnitude greater than those predicted from equilibrium reaction kinetics, but could be explained by a corrosion process with the container material.. Further data, including measurement of vapor pressures and material removed up to high burnup, would be desirable. Other breeders may also have significant vapor pressures and scoping tests could be useful.

3.4 Examples of Recent Progress

The FINESSE study [74,55-57], carried out in the U.S. with participation of specialists from Canada, Europe and Japan has analyzed and quantified the important fusion technology issues and defined the major experiments and facilities required to resolve these issues. A test sequence for the major solid breeder blanket-tasks developed as part of the study is shown in Fig. 27. In time, there is a progressive increase on the level of integration of the experiments. Much of the recent progress has been achieved by obtaining fundamental property data and by performing fission experiments which can be classified into two areas: (1) solid breeder material irradiation experiments, and (2) in-situ tritium recovery experiments. Since experiments can never cover all possible ranges of relevant parameters, a modelling effort is required parallel to the experimental program to interpret experiments and to enable interpolation between and extrapolation beyond available experimental data. Furthermore, models are the primary tools for design.

Properties

The property data base on the major solid breeders has been considerably extended. A summary of the overall properties of solid breeders and Be can be found in Ref. [54]. A more thorough summary of the mechanical properties of Li_2O, Li_4SiO_4, $LiAlO_2$ and Be is given in Ref.[83] while Ref. [84] covers in details the physical and thermal transport properties of lithium ceramics. The thermodynamics and tritium related properties have also been measured and can be found in a number of references such as [54,82,85-87]. Experimental measurements of effective thermal conductivities to reproduce a Be packed bed configuration in conjunction with the proposed control of the Be region thermal conductivity for power variation accommodation for ITER[88] have recently been made.

Fission Reactor Experiments

(1) Solid Breeder Material Irradiation Experiments: Table 9 summarizes the material irradiation experiments completed and active worldwide since 1984. Solid breeder materials have been irradiated in both thermal and fast reactors to investigate the impact of irradiation on stability, tritium and helium retention, and thermal conductivity. Relatively low lithium burnups when compared to present commercial designs were achieved, except for FUBR-1B whose burnup is comparable to multiplied blankets. Among the findings is the considerable swelling of Li_2O as opposed to the ternary ceramics, $LiAlO_2$ in particular. BEATRIX-II will also consider the compatibility of lithium ceramic in contact with Be.

(2) In-situ Tritium Recovery: Worldwide (except USSR) completed and on-going in-situ tritium recovery experiments are summarized in Table 10. In many experiments, such as TRIO[89], MOZART[65], and VOM-23H[90], addition

of hydrogen to the helium purge gas was found to substantially boost the tritium release by effectively causing a reduction in the tritium surface inventory. From the MOZART experiment [65] as an example, Li_2O was found to have excellent tritium release behavior as evidenced by Fig. 28 which shows the tritium residence time for MOZART samples of Li_2O, Li_2ZrO_3 and $LiAlO_2$ as a function of temperature for the case of an helium purge with 0.1% H_2. Li_2ZrO_3 performance is close to that of Li_2O while $LiAlO_2$ is found to have poorer tritium release characteristics.

From the LISA experiment [91], Li_4SiO_4 exhibits reasonably good tritium release characteristics but not as good as the MOZART Li_2O and Li_2ZrO_3 samples. Note, however, that specifics such as the sample microstructure, for example, can play an important part in the release behavior and attempts at generalizing results must be done very carefully. This is where modeling plays a key role to enable extrapolation of results from specific cases to a range of parameters.

Modeling

A fundamental part of the R&D plan for solid breeders is the development of predictive capabilities which are necessary to design, construct and operate the solid breeder blanket component. This requires a highly interactive program of theory, modeling and experiments. Theory and modeling are both used in planning and designing experiments to maximize their benefits, and in understanding experimental data and extrapolating them to different parameter ranges of interest.

Recent progress in modeling includes (1) modeling of tritium transport in solid breeders, (2) modeling of purge gas behavior and (3) modeling of pebble bed conductance as a means of controlling the solid breeder temperature.

Tritium Modeling: Models have focused on the processes of tritium diffusion through the grain and desorption from the grain surface and have been able to reproduce reasonably well the tritium release observed experimentally particularly for temperature transients [90,92,93]. A comprehensive model for tritium transport is MISTRAL[93] which includes the processes of tritium diffusion through the grain and grain boundary, adsorption from the bulk, desorption to the pores (and adsorption from the pores), and diffusion along interconnected porosity. The key processes are the surface processes (adsorption and desorption) which need to be correctly included in the model in particular for modeling purge hydrogen concentration transients.

Purge Modeling: Modeling of the helium purge characteristics for flow through a solid breeder or Be packed bed using the Modified Darcy's equations [66] showed the constraint due to the pressure drop in particular for low porosity cases.

The flow rate design window will be dictated by the maximum allowable pressure drop on the upper end and by the maximum allowable tritium partial pressure based on permeation limits on the lower end.

Packed Bed Conductance: Modeling the effective thermal conductivity of solid breeder and Be regions is becoming increasingly important in particular when considering the need for solid breeder blankets to accommodate power variations. A packed bed configuration offers the potential of varying the effective conductivity through purge flow rate, pressure and/or composition changes. several models exist for estimating the effective conductivity of a packed bed as a function of various parameters (e.g. Refs. [94,95]). However, in the case of high conductivity Be particle packed bed, parameters such as the contact area and surface characteristics become particularly important. A modeling effort is underway to build up on past efforts and to develop a model particularly suited for high conductivity particle packed beds [88[.

Thermomechanics Experiments: Unfortunately, very little effort has been spent on the purely thermechanical testing of solid breeder blankets due mainly to resource limitations and perceived priorities. The available resources have been focused mostly on tritium related experiments which are thought to address key issues for solid breeders. One of the few purely mechanical tests is described in Ref.{96} and addresses the structural response of a NET canister type blanket elements under accidental overpressure.

REFERENCES;

1. M.A. Abdou, et al., "FINESSE: A study of the issues, Experiments, and Facilities for Fusion Nuclear Technology Research and Development (Interim Report), "PPG-821, UCLA-ENG-84-30, October 1984.

2. J.K. Garner and M.A. Abdou "Uncertaintities in Liquid Metal Fusion Blanket Design Windows," Fusion Tech. 10(3) Part 2, Nov. 1986, pp. 837-847.

3. G. Casini, "Thermal and Structural Design Issues of Breeding Blankets for Testing in the Next European Tours," Fusion Eng. & Design 6(2), 1988, pp. 95.

B.F. Picologlou, Y.S. Cha, and S. Majumdar, "Lithium-Cooled Blankets for Advanced Tokamaks," Fusion Tech. 10(3) Part 2, Nov. 1986, pp.848-853.

5. S. Malang, et al., "Self-Cooled Liquid-Metal Blanket Concept," Fusion Technology, 14(3), Nov. 1988, 1343.

6. A. Majid and M.A. Abdou, "Thermomechanical Aspects of the Liquid Metal Cooled Limiter," Fusion Tech. 15(2) Part 2, March 1989, pp. 1192-1195.

7. V.N. Dem'yanenko, et al., "Liquid Metal in the Magnetic Field of Tokamak Reactor," Magnetohydrodynamics, No. 1, 1998.

8. W.M. Wells, "A System for Handling Divertor Ion and Energy Flux Based on a Lithium Droplet Cloud," Nuclear Technology/Fusion, 1(1) 1981.

9. R.W. Moir, "Rotating Liquid Blanket with No First Wall for Fusion Reactors," Fusion Technology, 15(2) Part 2, March 1989, pp. 674-679.

10. A.M. Hassanein and D.L. Smith, "Evaluation of Liquid Metal Protection of a Limiter/Diverto in Fusion Reators," Fusion Technology, 15(2) Part 2, March 1989, pp. 1196-1202.

11. B. Badger, et al., "UWMAK-I: A Wisconsin Toroidal Fusion Reactor Design, "UWFDM-68, Nov. 20, 1973.

12. "Tokamak Power Systems Studies," ANL/FPP-85-2.

13. D. Ehst, et al., "Tokamak Power Systems Studies-FY1986: A Second Stability Power Reactor," ANL/FPP-86-1, 1986.

14. J.S. Walker and B.F. Picologlou, "Comparison of Three MHD Flow Control Methods for Self-Cooled Liquid Metal Blankets," Fusion Tech. 10(3) Part 2, Nov. 1986, pp. 866-871.

15. B.F. Picologlou, C.B. Reed, T.Q. Hua, L. Barleone, H. Kreuzinger, and J.S. Walker, "Experimental Investigations of MHD Flow Tailoring for First Wall Coolant Channels of Self-Cooled Blankets," Fusion Technology, 15(2) Part 2, March 1989, pp. 1180-1185.

16. J.C.R. Hunt, "Magnetohydrodynamic Flow in Rectangular Ducts," J. Fluid Mech. 21(4) 1965, pp. 577-590.

17. H. Branover, et al., "Turbulence and the Feasibility of Self-Cooled Liquid Metal Blankets for Fusion Reactors," Fusion Tech 10(3) Part 2, Nov. 1986, pp. 822-829.

18. C.B. Reed and B.F. Picologlou, "Sidewall Flow Instabilities in Liquid Metal MHD Flow Under Blanket Relevant Conditions," Fusion Technology, 15(2) Part 2, March 1989, pp. 705-715.

19. K. Fujimura, "Stability of a MHD Flow Through a Square Duct," UCLA-FNT-023, April 1989.

20. B.F. Picologlou, C.B. Reed, T.Q. Hua, and A.S. Lavine, "The Design of a Heat Transfer Liquid Metal MHD Experiment for ALEX," Fusion Technology, 15(2), Part 2, March 1989, pp. 1186-1191.

21. L. Blumeau, et al., "Liquid Metal MHD Energy Conversion in Fusion Reactors," Fusion Tech. 10(3) Part 2, Nov. 1986, pp. 914-921.

22. C.B. Reed, B.F. Picologlou, and P.V. Dauzvardis, "Experimental Facility for Studying MHD Effects in Liquid Metal Cooled Blankets, "Fusion Technology, Vol. 8, July 1985.

23. L. Barleone, et al., "Experimental and Theoretical Work on MHD at Kernforschungszentrum Karlsruhe, The MEKKA Program, "Proc. of the IUTAM Symposium on Liquid Metal MHD, May 16-20, 1988, Riga USSR.

24. Ja. Dekeyser, et al., "Status of the Liquid Metal Breeder Research Programme at CEN/SCK-MOL (Belgium), "Proceedings of the IAEA 4th Technical Committee Meeting and Workshop on Fusion Reactor Design and Technology, Yalta, USSR, May 25-June 6, 1986.

25. T. Ida, A. Serizawa, O. Takahashi, and I. Michiyoshi, "Heat Transfer and Flow Properties in Liquid-Metal-Gas Two-Phase MHD Flow," JSME No. 864-2 (1986) 65-68.

26. J.C.R. Hunt and R. Hancox, "The Use of Liquid Lithium as Coolant in a Toroidal Fusion Reactor. Part I: Calculation of Pumping Power, 'CML-R115, 1971., see also M.A. Hoffman, and G.A. Carlson, "Calculation Techniques for Estimating the Pressure Losses for Conducting Fluid Flows in Magnetic Fields," UCRL-51010, 1971., see also M.A. Hofman, "Magnetic Field Effects on the Heat Transfer of Potential Fusion Reactor Coolants," UCRL-73993, June 23, 1972.

27. K. Taghavi, M.S. Tillack, and H. Madarame, "Special Features of First-Wall Heat Transfer in Liquid-Metal Fusion Reactor Blankets," Fusion Technology, Vol. 12, No. 1, July 1987.

28. R.J. Holroyd and J.S. Walker, "A Theoretical Study of the Effects of Wall Conductivity Non-uniform Magnetic Fields and Variable Area Ducts on Liquid Metal Flows at High Hartmann Number," J. Fluid Mech., Vol. 84, pp. 471-495 (1978).

29. G.S.S. Ludford and J.S. Walker, "Current Status of MHD Duct Flow," from MHD-Flows and Turbulence II, ed. by H. Branover and A. Yakhot, Israel Universities Press, Jerusalem, 1980.

30. A.G. Kulikovski, "Slow Steady Flows a Conducting Fluid at Large Hartmann Numbers," Fluid Dynamics, 3,2(1968)3-10.

31. B. Singh and J. Lal, "Finite Element Method in Magnetohydrodynamic Channel Flow Problems," International Journal for Numerical Methods in Engineering, Vol. 18, 1104 (1982).

32. J.I. Ramos and N.S. Winowich, Magnetohydrodynamic Channel Flow Study," Phys. Fluids 29(4), April 1986, pp. 992-997.

33. N.S. Winowich and W.F. Hughes, "A Finite-Element Analysis of Two-Dimensional MHD Flow," from Liquid Metal Flows and Magnetohydrodynamics, ed. by H. Branover, P.S. Lykoudis, and A. Yakhot, 1983, pp. 313-322.

34. M.S. Tillack, "Application of the Core Flow Approach to MHD Fluid Flow in Geometric Elements of a Fusion Reactor Blanket," IUTAM Symposium on Liquid Metal Magnetohydrodynamics, Riga USSR, 16-20, May 1988.

35. T.Q. Hua and J.S. Walker, B.F. Picologlou, and C.B. Reed, 'Three Dimensional Magnetohydrodynamic Flows in Rectangular Ducts of Liquid-Metal-Cooled Blankets," Fusion Tech. 14(3), Nov. 1988, 1389.

36. K. McCarthy, M.A. Abdou, and M.S. Tillack, "Analysis of Liquid Metal MHD Flow Using an Iterative Method to Solve the Core Flow Equations," International Symposium on Fusion Nuclear Technology, April 1988.

37. C.N. Kim, "Development of a Numerical Method for Full Solution of Magnetohydrodynamic Flows and Application to Fusion Blankets," UCLA Ph.D. Dissertation, under M.A. Abdou, Jan. 1989.

38. A. Sterl, "Numerical Simulation of Magnetohydrodynamic Liquid-Metal-Flow in Rectangular Ducts at High Hartmann Number," Karsruhe University

Ph.D. Thesis, 1989.

39. M. Tillack, A. Ying, and H. Hashizume, "The Effect of Magnetic Field Alignment on Heat Transfer in Liquid Metal Blanket Channels, 'UCLA-FNT-24, March 1989.

40. T.Q. Hua, and B.F. Picologlou, "Heat Transfer in Rectangular First Wall Coolant Channels of Self-Cooled Blankets," Fusion Technology, 15(2) Part 2, March 1989, pp. 1174-1179.

41. M.A. Abdou, et al., "Blanket Comparison and Selection Study," - interim report, ANL/FPP-83-1, Oct. 1983.

42. D.L. Smith, et al., "Blanket Comparison and Selection Study-Final Report," ANL/FPP-84-1, Sept. 1984.

43. P. Gherson and P.S. Lykoudis, "Local Measurements in Two-Phase Liquid-Metal Magneto-Fluid-Mechanic-Flow," J. Fluid Mech. 147 (1984)81-104.

44. T.N. Aitov, A.I. Kalyutik, and A.V. Tananaev, "Numerical Analysis of Three-Dimensional MHD Flow in Channel with Abrupt Change of Cross Section," Magnetohydrodynamics, No. 2, pp. 123-130, April-June 1983.

45. R.A. Gardner and P.S. Lukoudis, "Magneto-Fluid-Mechanic Pipe Flow in Transverse Magnetic Field: Part 2, Heat Transfer, "J. Fluid Mech., 48, pp. 129-141, 1971.

46. H. Branover and P. Gershon, "Experimental Investigation of the Origin of Residual Disturbances in Turbulent MHD Flows After Laminarzation," J. Fluid Mech., 94, pp. 629-647, 1979.

47. M.A. Abdou, et al., "Fusion Reactor Design IV: Report on the Fourth IAEA Technical Committee Meeting and Workshop, Yalta, USSR, May 26 - June 6, 1986, "Nuclear Fusion 26(10) 1986, pp. 1377-1428.

48. C.N. Kim and M.A. Abdou, "Numerical Method for Fluid Flow and Heat

Transfer in Magnetohydrodynamic Flow," Fusion Technology, 15(2) Part 2, March 1989, pp. 1163-1168.

49. H. Madamrame and H. Tokoh, "Development of Computer Code for Analysing Liquid Metal MHD Flow in Fusion Reactor Blankets, (I)," Journal of Nuclear Science & Technology, Vol. 25, No. 3, March 1988, pp. 233-244.

50. Yu. B. Kolesnikov, "Two-Dimensional Turbulent Flow in a Channel with Inhomogeneous Electrical Conductivity at the Walls," Magnetohydrodynamics 8(3), July-Sep. 1972, pp. 308-312.

51. B. Lehnert, "An Instability of Laminar Flow of Mercury Caused by an External Magnetic Field," Proc. Royal Soc., A., Vol 233, Dec. 1955.

52. G. Fabris, et al., "High-Power-Density Liquid-Metal MHD Generator Results," Proc. 18th Symp. on Engineering Aspects of Magnetohydrodyamics, 1979, pp. D2.2.2.-6.

53. P.F. Dunn, et al., "High-Power-Density Liquid-Metal MHD Generator Experiments, "Proc. 18th Symp. on Egineering Aspects of Magnetohydrodynamics, 1979, pp. D2.2.7-12.

54. M.A. Abdou, et al., "A Study of the Issues and Experiments for Fusion Nuclear Technology," UCLA-ENG-86-44, Jan. 1987.

55. M.A. Abdou, et al., "A Study of the Issues and Experiments for Fusion Nuclear Technology," Fusion Technology, Vol. 8, pp. 2595-2645, (Nov. 1985).

56. M.A. Abdou, et al., "Technical Issues and Requirements of Experiments and Facilities for Fusion Nuclear Technology," Nuclear Fusion, Vol. 27, No. 4 (1987).

57. M.A. Abdou, et al., "Modeling, Analysis and Experiments for Fusion Nuclear Technology, Fusion Engineering and Design, Vol. 6, pp. 3-64 (1988).

58. Y. Gohar, et al., 'Solid Breeder Blanket,' as part of U.S. Contributions to the Homework of ITER, Argonne National Laboratory, Feb. 1989

59. M.A. Abdou, et al., 'Summary of the ISFNT Workshop on the International Thermonuclear Reactor,' Fusion Technology Vol. 14, p. 1399, Nov. 1988

60. M. Dalle Donna, et al., 'Pebble-Bed Canisters: The Karlsruhe Ceramic Breeder Blanket Design for the next European Tour US,' Fusion Technology, Vol. 14, p. 1357, Nov. 1988

61. G. Chevereau, 'Adaptation to NET of a Beryllium Canister Blanket Concept, 'Novatome-Framatome, CEA/Saday, France

62. V. Zampaglione et al, "IL MANTELLO - A scoping Study Using Solid Breeders in a Gas cooled Tokamak Blanket with NET Physics, 'Centro Richerche Energin Frascati, Italy

63. ITER SHIELD & BLANKET WORK PACKAGE REPORT, DRAFT, U.S. ITER Nuclear Group, ANL/FPP/88-1, Argonne National Laboratory, May 1988

64. M.A. Abdou et al, 'Deuterium-Tritium Fuel self-sufficiency in Fusion Reactions, 'Fusion Technology Vol. 9, p250, March 1986

65. M. Briec et al, "The MOZART Experiment: In-Pile Tritium Extraction from Li_2O, $LiAlO_2$, Li_2ZrO_3, 'presented by N. Roux at the Solid Breeder Working Group Meeting, October 13-14, 1988, Park City, Utah

66. K. Fujimura, et al., 'Analysis of Helium Purge flow in a Solid Breeder Blanket, 'presented at the International Symposium on Fusion Nuclear Technology, April 10-15, 1988, Tokyo, Japan

67. A.R. Raffray, et al., 'Material Form for Be, 'as part of U.S. Contributions to the Homework for ITER, Argonne National Laboratory, Feb. 1989

68. M.C. Billone, H. Hashizume et al, 'Thermal-Mechanical Analyses of the Be Multiplier Zones, 'as part of U.S. Contributions to the Homework for ITER, Argonne National Laboratory, Feb. 1989

69. Bauer and Schlunder International Chemical Engineering, Vol. 18, No. 2, [1978] p. 189

70. M.S. Kazimi et al., "Thermal Limits for Passive Safety of Fusion Reactors," Fusion Technology, Vol. 15, Number 2, Part 2B, p. 827, March 1989

71. M.A. Abdou, et al, 'A Helium-cooled Solid Breeder Concept for the Tritium-ProducingBlanket of the International Thermonuclear Reactor,' Fusion Technology, vol. 15, No. 2, Part 1, p. 166, March 2,1989

72. M.A. Abdou and D. Graumann, "The Choice of Collant in Commercial Tokamak Power Plants," Proc. 4th Topcl Mtg on the Tech. of Cont. Nucl. Fusion, Vol. III, (1981)

73. Z.R. Gorbis, et al., 'LOCA Study for a Helium-Cooled Solid Breeder Design for ITER,' Fusion Technology, Volume 15, Number 2, Part 2B, P. 821, March 1989

74. M.A. Abdou, et al., "Technical Issue and Requirements and Facilities for Fusion Nuclear Technology (FINESSE Phase I Report), "PPG-909, UCLA-ENG-85-39, University of California, Los Angeles (1985)

75. M.A. Abdou, et al, "A Demonstration Tokamak Power Plant Study (DEMO), 'ANL/FPP-82-1, Argonne National Laboratory, September 1982

76. C. Baker, et al., 'STARFIRE; A Commercial Tokamak Fusion Power Plant Study,' ANL/FPP-80-1, Argonne National Laboratory, September 1980

77. O. Chopra and D.L. Smith, 'compatibility Studies of Structural Alloys with Solid Breeder Materials,' in Alloy Devel. for Irr. Perf. Semiannual Prog. Report for Period Ending Sept. 30, 1983, DOE/ER/0045/11, U.S. Dept. of Energy, March 1984

78. Pulham R., W.R. Watson and J.S. Collinson, "Chemical compatibility between Lithium Oxide and Transition Metals,' Proc. 3rd Top. Mtg. on fusion Reactor Materials, Albuquerque, New Mexico, September 12-22, 1983

79. D.L. Porter, et al, 'Neutron Irradiation and Compatibility Testing of Li_2O 'Journal of Nuclear Material, 122 & 123 (1984), p. 929

80. G.W. Hollenberg, "The Effect of Irradiation on Four Solid Breeder Materials,' First Int. Conf. on Fusion Reactor Materials, Tokyo, Japan, December 3-6, 1984

81. T.J. McCarville, et al, 'Technical Issues for Beryllium Use in Fusion Blanket Applications, 'UCID-20319, Lawrence Livermore National Laboratory, January 1985

82. A.K. Fischer and C.E. Johnson, 'Thermodynamics of Li_2O and Other Breeders for Fusion Reactors,' J. Nucl. Mat. 133/134, 184 (1985)

83. M.C. Billone and W.T. Grayhack, 'Summary of Mechanical Properties Data and Correlations for Li_2O, Li_4SiO_4, $LiAlO_2$, and Be,' ANL/FPP/TM-218, Argonne National Laboratory, April 1988

84. D.J. Suiter, 'Lithium Based Oxide Ceramics for Tritium Breeding Applications,' MDC E2677/UC-20,McDonnell Douglas, June 1983

85. K. Okuro and H. Kudo, 'Tritium Diffusivity in Lithium-Based Ceramic Breeders Irradiated with Neutrons,' presented at International Symposium on fusion Nuclear Technology, April 1988, Tokyo, Japan

86. A.K. Fischer and C.E. Johnson, 'Measurements of Adsorption in the $LiAlO_2$-H_2O (g) System," Fusion Technology, vol. 15, p. 1212, March 1989

87. H.R. Ihle and C.H. Wu, "Chemical Thermodynamics of fusion Reactor Breeding Materials and their Interaction with Tritium," Journal of Nuclear Materials 130 (1985) 454, North-Holland, Amsterdam

88. Z.R. Gorbis, et al., "Thermal Resistance Gaps for Solid Breeder Blankets Using Packed Beds," Fusion Technology, Vol. 15, p. 695, March 1989

89. R.G. Clemmer, et al., "TRIO Experiment," ANL-84-55, Argonne National Laboratory, September 1984

90. T. Kurasawa, et al., "In-Pile Tritium Release Behavior from Lithium Aluminate and Lithium Orthosilicate of the VOM-23 Experiment," Journal of Nuclear Materials, 155-157 (1988) 544-548, North-Holland, Amsterdam

91. H. Werle, et al., "The LISA 1 Experiment: In-Situ Tritium Release Investigations," presented at the second International Conference on Fusion Reactor Materials, April 1986, Chicago

92. J. Kopasz et al, "Modeling of Tritium Behavior in Ceramic Breeder Materials," ANL/FPP/TM-231, Argonne National Laboratory, November 1988

93. A.R. Raffray, G. Federici, et al., "MISTRAL-A comprehensive Model for Tritium Transport in Solid Breeders," presented at the second International Specialists workshop on Modeling Tritium Behavior in Ceramic Fusion Blankets, Indianapolis, April 1989

94. R.O.A.Hall and D.G. Martin, "The Thermal conductivity of Powder Beds. A Model, some Measurements on UO^2 vibrocompacted Microspheres, and their Correlation," Journal of Nuclear Materials 101(1981) 172-183, North-Holland Amsterdam

95. M.J. Ades and K.L. Peddicord, "A Model for Effective Thermal Conductivity of Unrestructured Sphere-Pace fuel," Nuclear Science and Engineering: 81, 540-550 (1982)

96. E. Wehner, et al., "Canister Type Blanket Elements for NET under accident Overpressure-Theoretical and Experimental Investigations," Fusion Engineering and Design 6 (1988) 69-78

LIST OF FIGURES

LIST OF FIGURES

Fig. 22.(b) Variation of maximum gas-phase conductance (d=o) with temperature. [41]

Fig. 23. Allowable power increase as a function of the predictability and controllability of the effective thermal conductivity of the Be region of the solid breeder blanket for ITER of Fig. 12

Fig. 24. Zirconium packed bed effective thermal conductivity (normalized to the gas thermal conductivity) as a function of gas pressure for different filling gases. [69]

Fig. 25. Temperature history following a LOCA in first wall and shield for an example Li_2O/He/HT_9 blanket and a first wall load of 5MW/m^2. [70]

Fig. 26. Temperature history of the first wall of a Li_4SiO_4/He Blanket following a LOCA for different purge velocities (based on maximum afterheat values) (conditions: thermal radiation between outboard regions only; flowing purge; conduction through He). [73]

Fig. 27. Test Sequence for Major Solid Breeder Blanket Tasks. [56]

Fig. 28. Tritium residence time for samples of Li_2O, $LiAlO_2$ and Li_2ZrO_3 as a function of temperature from the MOZART experiment. [65]

Table 9 Completed and On-going Solid Breeder Material Irradiation Experiments in USA, Europe, Japan and Canada

Experiment	Ceramic	Grain Size (μm)	Density (%TD)	Temperature (°C)	Li Burn-up (Max at %)	Reactor	Time Frame
Closed Capsule							
ORR (US)	Li_2O	~47	70	750, 850, 1000	0.05	ORR	
TULIP	Li_2O	50	87	600	3	EBR II	84
EUBR 1A (US)	Li_2O	6	85	500, 700, 900	1.5	EBR II	84/85
	$LiAlO_2$	<1	85, 95	500, 700, 900	3		84/85
	Li_4SiO_4	2	85	500, 700, 900	2		84/85
	Li_2ZrO_3	2	85	500, 700, 900	2		84/85
EUBR 1B (US)	Li_2O	~5	60, 80	500, 700, 900	5	EBR II	85/89
	Li_2O	<5	80	500-700/1000			
	$LiAlO_2$	~5-10	80	500, 700, 900	9		85/89
	(sphere pac)		80	500-700/1000			
	Li_4SiO_4	~5	80	400-500	9		85/89
	Li_8ZrO_6	<5	80	600-700	7		85/89
	Li_2ZrO_3	~5	85	520-620	7		85/89
ALICE (France)	$LiAlO_2$	0.35-13	71-84	400, 600		OSIRIS	85/86
DELICE (FRG)	Li_2SiO_3		65, 85	400, 600, 700	0.02	OSIRIS	85/86
	(Li_4SiO_4)		95				
ORDALIA (Italy)	$LiAlO_2$	0.4-2.0-10	80	600, 700		OSIRIS	86/87
EXOTIC	Li_2SiO_3		80	400, 600		HFR	85/86
(Neth./UK/Belgium)	Li_2O						85/86
	$LiAlO_2$	30	80				85/86
	Li_2ZrO_3						85/86
CRETE (Canada)	$LiAlO_2$	~1	80, 90	100		NRU	85/86
BEATRIX II (IEA)	Li_2O		85, 100	390-425	4	HFR	89-90
	Li_2O/Be						
	Li_2ZrO_3/Be						
	$LiAlO_2$/Be						
	Li_4SiO_4/Be						

Table 10 Completed and On-going In-Situ Tritium Recovery Experiments for Solid Breeders in USA, Europe, Japan and Canada

Experiment	Ceramic	Grain Size (μm)	Density (%TD)	Temperature (°C)	Li Burn-up (Max at %)	Reactor	Time Frame
TRIO (US)	$LiAlO_2$	0.2 (50 μm particles, 0.9 cm thick annular pellet)	65	400 700	0.2	OHR	84-85
VOM 15H (Japan)	Li_2O	<10	86	480 760	0.24		84
VOM 21H (Japan)	Li_2O		89-95	485 900	0.86	JRR-2	84/85
VOM 22H (Japan)	Li_2O	10 (0.5 cm spheres)	85	350 900	0.5	JRR-2	85/86
	$LiAlO_2$	4 (0.4 cm spheres)	77	430 900	1.7		
VOM 23H (Japan) (BEATRIX I)	$LiAlO_2$	0.5 (0.4 cm dia. rods)	77	600 850	0.26	JRR-2	86
	Li_4SiO_4	14 (0.4 cm spheres)	90	500 900	0.28		
VOM 22/23 (Japan)	Li_2O	(1.1 cm pebbles)		400 900	0.04		
	$LiAlO_2$	(1.1 cm pebbles)		400 900	0.1		
VOM 31H (Japan)	Li_2O	Single Crystal (0.8 cm dia.)	100	400 900	(121 FPD)	JRR-2	88/89
		13 (pellet)	89.5	400 900	(121 FPD)		
LILA (France)	$LiAlO_2$	1-30 (1 cm dia. pellet)	78	375 600	~0.02	SILOE	86
LISA (LIBG, France)	$LiAlO_2$	0.4	78	450 730		SILOE	86
	Li_2SiO_3	30 80	86 93	450 730			
	Li_4SiO_4	26 (1 cm diameter pellet)	94	450 730			

Table 10 (Cont.)

Experiment	Ceramic	Grain Size (μm)	Density (%TD)	Temperature (°C)	Li Burn-up (Max at %)	Reactor	Time Frame
EXOTIC (Neth./UK/Belgium) (I, II, III)	$LiAlO_2$	30, 8 (1.4 cm dia. pellet)	80, 95	400, 650	~0.4	HFR	86
	Li_2SiO_3	(1.4 cm dia. pellet)	50	400, 650	~0.4		86
	Li_2O	5	80	400, 650	<0.4		86/87
	Li_2ZrO_3	2	80	400, 650	<0.4		86/87
EQUILA (Italy)	$LiAlO_2$	0.4 2.0 10 (1 cm dia. pellet)	80	500, 700		SILOE	88/89
CRITIC (Canada)	Li_2O	60 (1 cm thick annular pellet)	90	400 900	0.15	NRU	86
EXOTIC IV	Li_2ZrO_3	5	80, 85	350 680	~4		86/87
	$Li_6Zr_2O_7$	5	80,	450 650	~4		
	Li_8ZrO_6	5	82	450 650	~4		
BEATRIX II Phase I (US, Japan, Canada)	Li_2O		85, 89	460 685	4	HFR	89/90
			89	450 900	4		
MOZART (France, US, Japan)	$LiAlO_2$		81, 92.7	300 680	Natural	MITUSIII	87/88
	Li_2ZrO_3		80	300 680			
	Li_2O		80	300 500			
SIBELIUS	Li_2O/Be		85	550		SILOE	89/90
	$LiAlO_2/Be$						
	Li_4SiO_4/Be						
	Li_2ZrO_3/Be						
BEATRIX II Phase II (US, Japan, Canada)	Li_2O		85	460 685	8	HFR	90/91
	Li_2ZrO_3		85	460 685	4		
	or Li_4SiO_4						

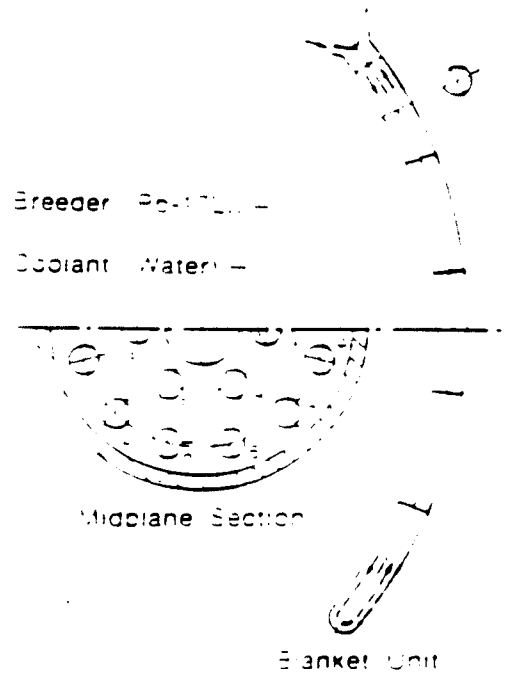

Fig. 1. Pb–17Li/water blanket – straight U-tube concept.

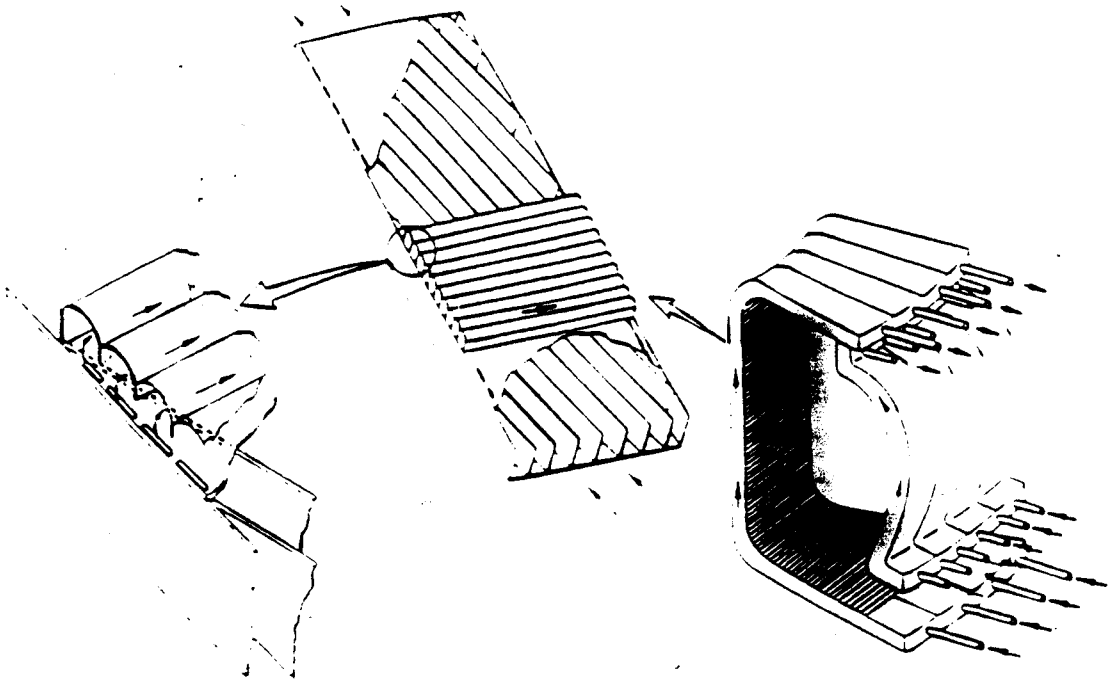

Fig. 2. Argonne National Laboratory reference design for the self-cooled liquid-metal blanket.

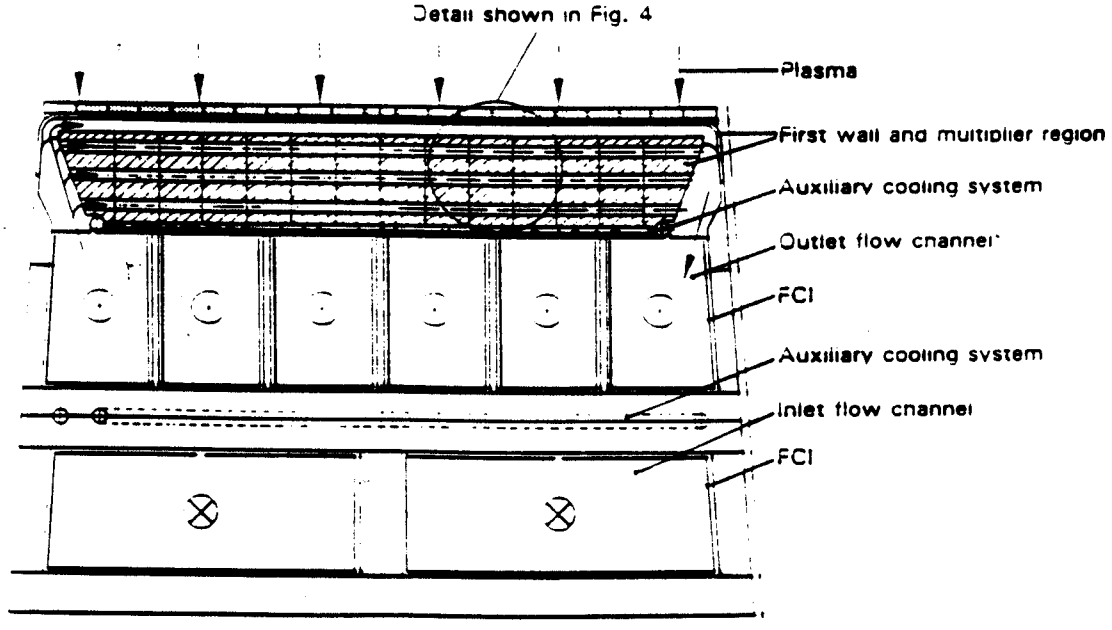

Fig. 3. Cross section of a liquid-metal-cooled blanket segment for NET.

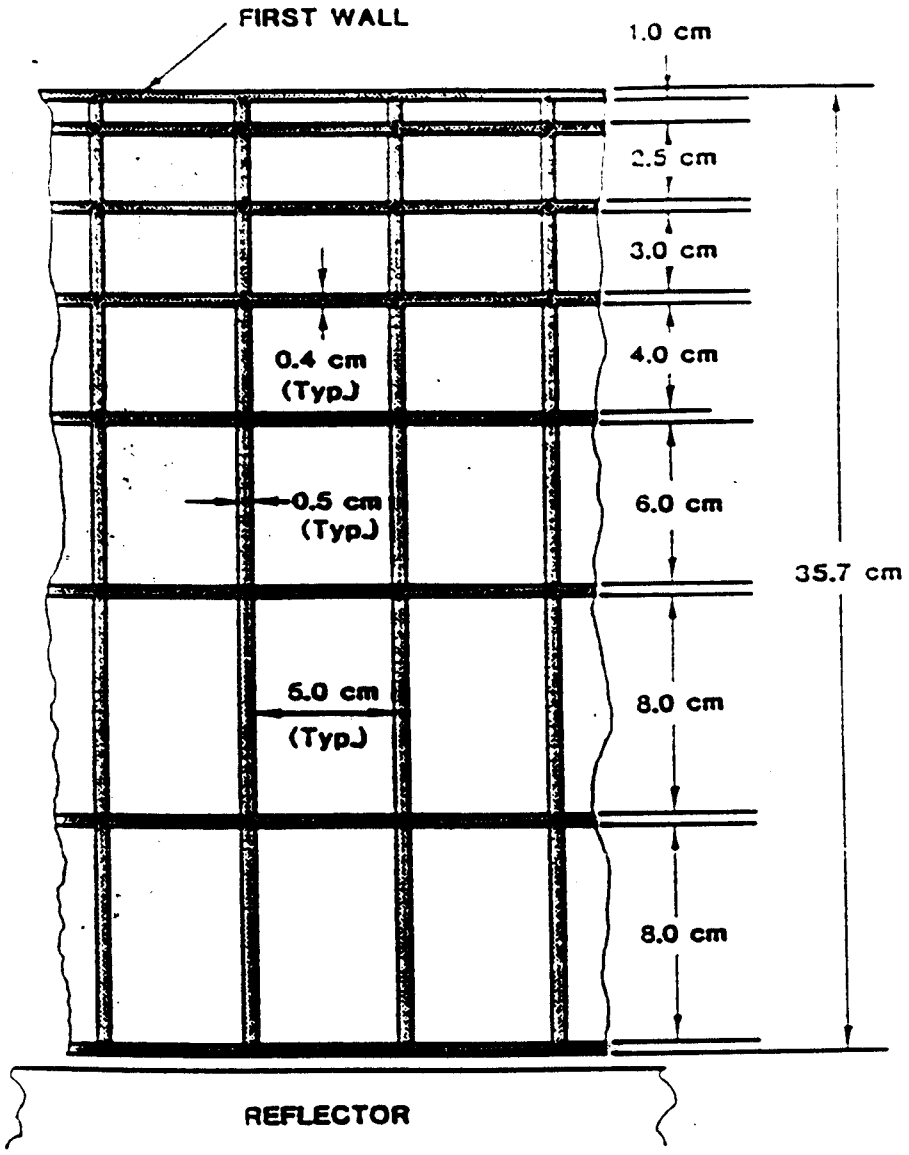

Figure 4 Cross section of the integrated first wall and breeding zone of the TPSS reactor. The dimensions shown are for the inboard blanket. The outboard blanket is similar but has a thinner breeding zone. The toroidal duct dimension of 5.0 cm corresponds to the first wall channel. For simplicity, the decrease of this dimension with radial position is not shown.

Figure 5 Liquid Metal Coolant Duct

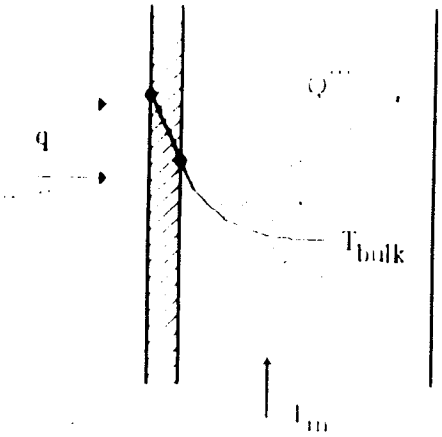

Fig. 7 General Design Strategies for Liquid Metal Cooled Blankets

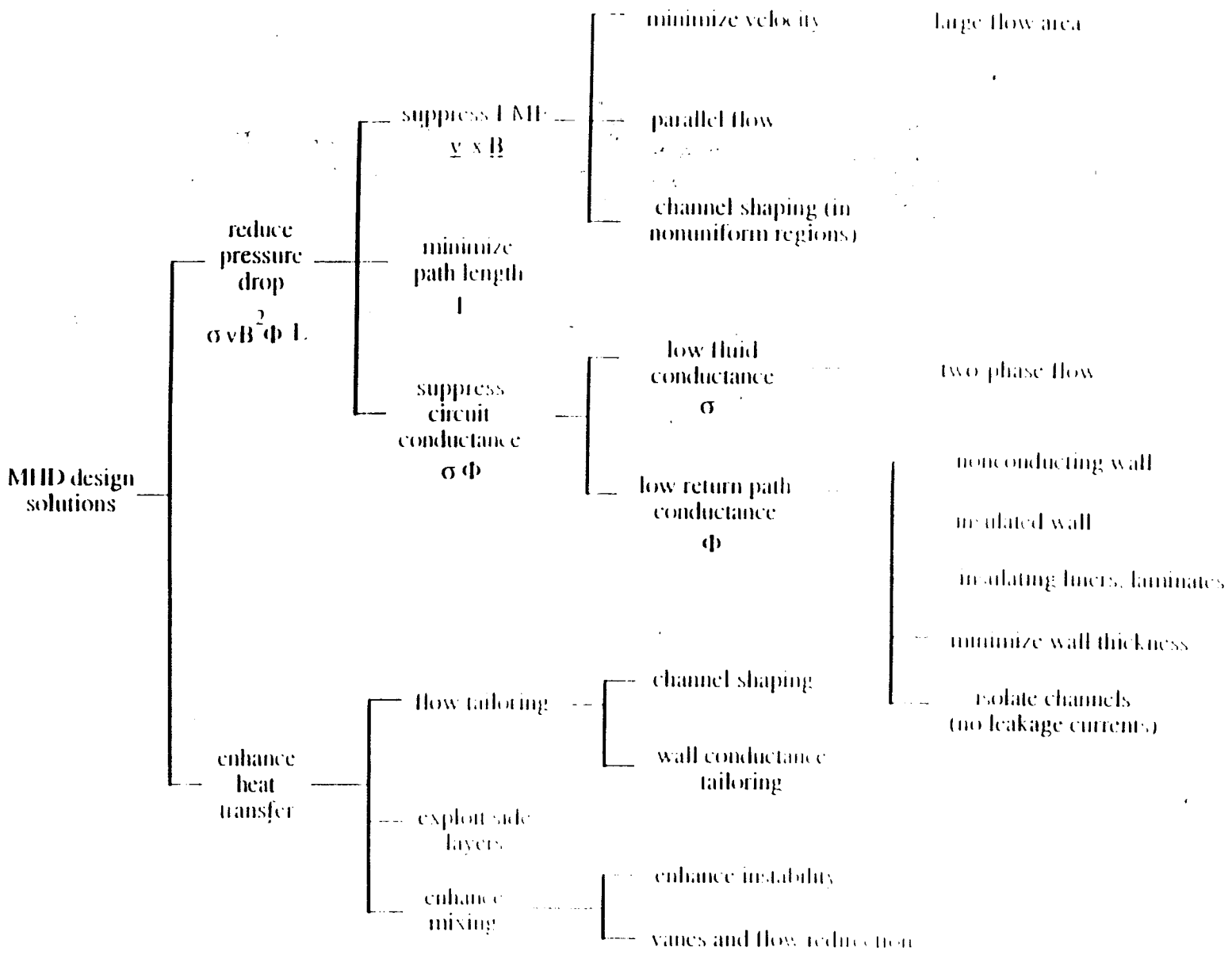

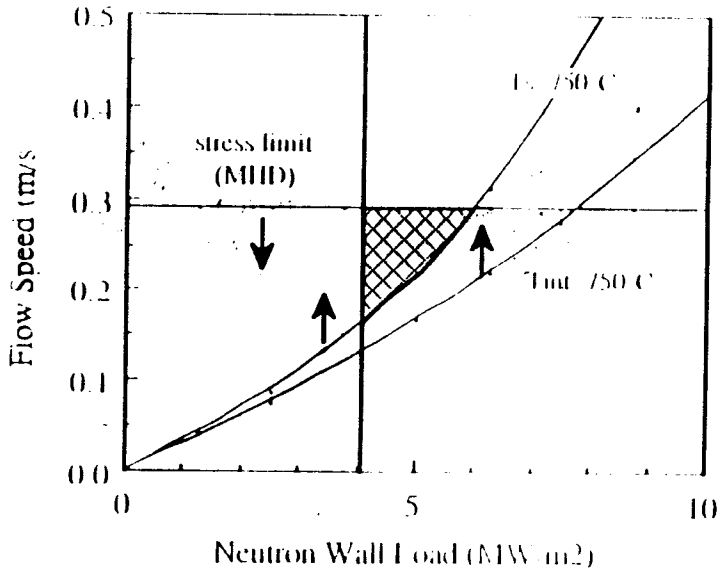

Fig. 6 Example of Design Window for a Li/V Blanket

Figure 8 Laminated structure for MHD pressure drop reduction

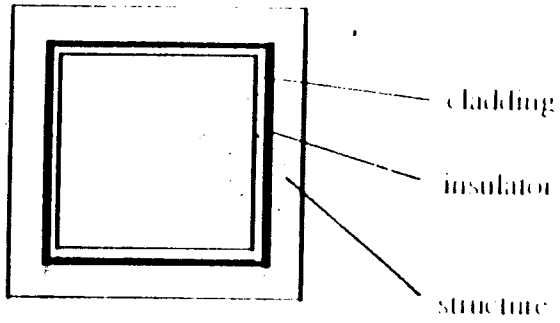

Figure : Parameter Ranges for MHD Facilities

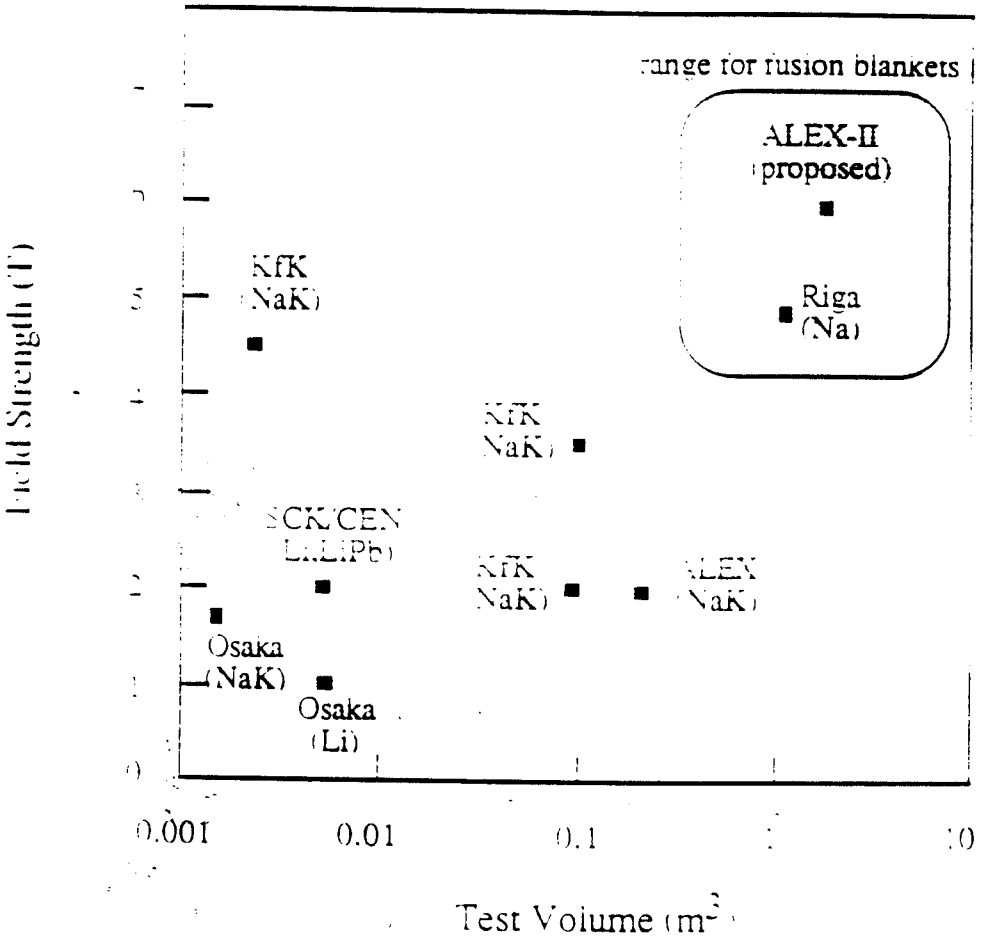

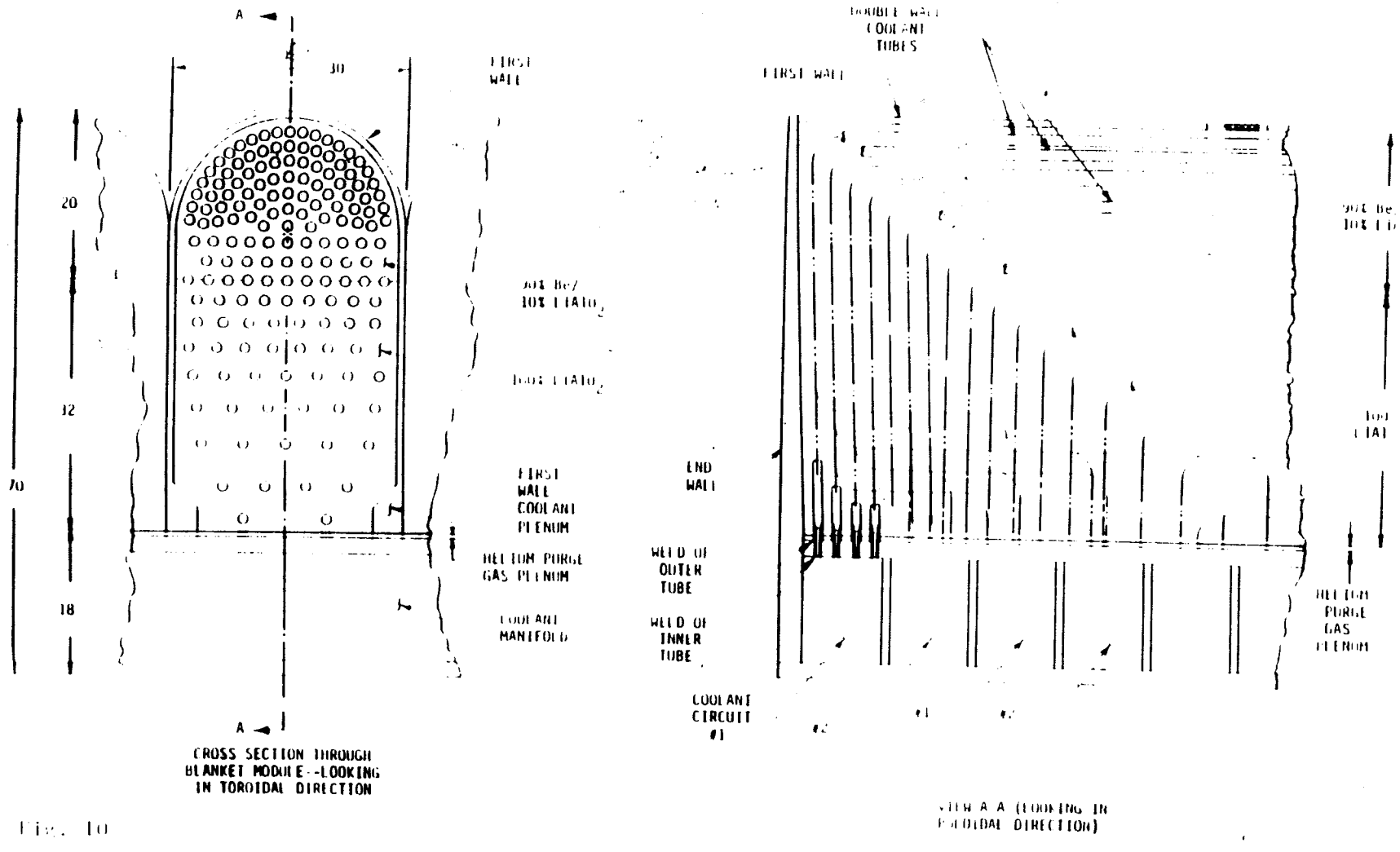

CROSS SECTION THROUGH BLANKET MODULE--LOOKING IN TOROIDAL DIRECTION

VIEW A A (LOOKING IN TOROIDAL DIRECTION)

(ALL DIMENSIONS IN CM)

FIG. 10

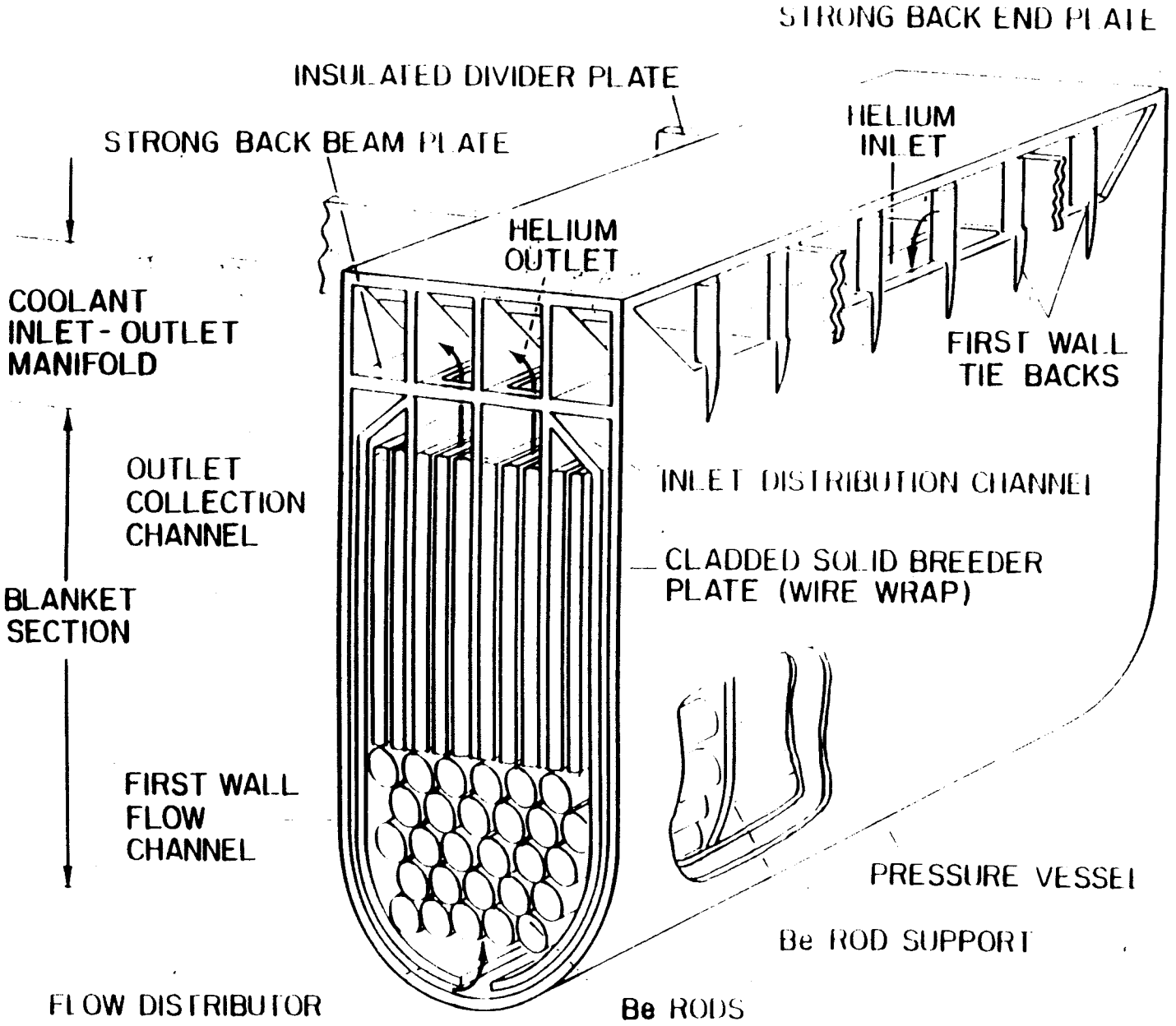
STRONG BACK END PLATE
INSULATED DIVIDER PLATE
STRONG BACK BEAM PLATE
HELIUM INLET
HELIUM OUTLET
COOLANT INLET - OUTLET MANIFOLD
FIRST WALL TIE BACKS
OUTLET COLLECTION CHANNEL
INLET DISTRIBUTION CHANNEL
CLADDED SOLID BREEDER PLATE (WIRE WRAP)
BLANKET SECTION
FIRST WALL FLOW CHANNEL
PRESSURE VESSEL
Be ROD SUPPORT
FLOW DISTRIBUTOR
Be RODS

Fig. 11

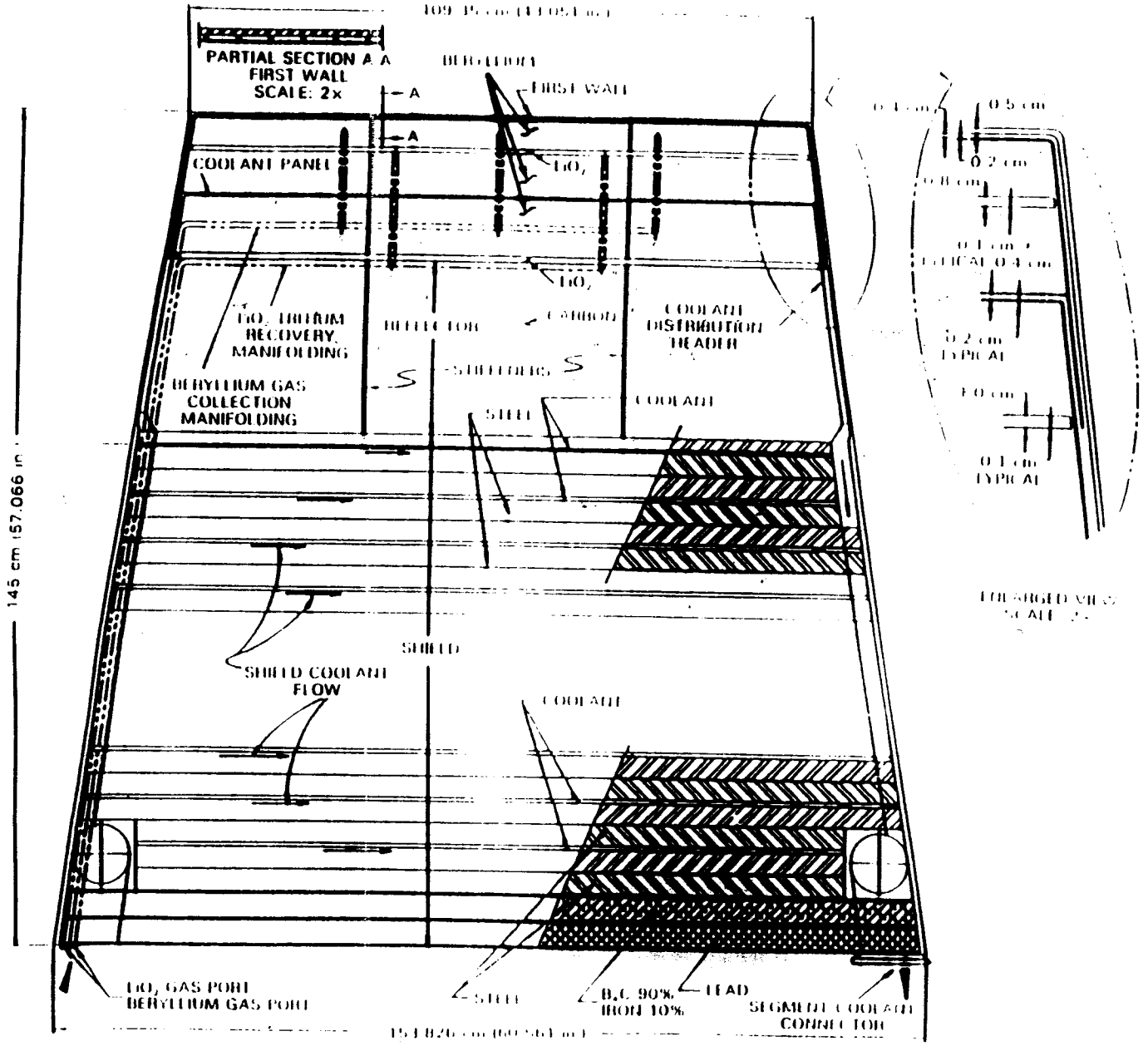
PARTIAL SECTION A-A
FIRST WALL
SCALE: 2x
A
A
BERYLLIUM
FIRST WALL
COOLANT PANEL
LiO_2
LiO_2
LiO_2 TRITIUM RECOVERY MANIFOLDING
BERYLLIUM GAS COLLECTION MANIFOLDING
BERYLLIUM
CARBON
COOLANT DISTRIBUTION HEADER
SHIELDING
STEEL
COOLANT
SHIELD
SHIELD COOLANT FLOW
COOLANT
LiO_2 GAS PORT
BERYLLIUM GAS PORT
STEEL
B_4C 90%
IRON 10%
LEAD
SEGMENT COOLANT CONNECTOR
145 cm (57.066 in)
0.5 cm
0.2 cm
0.8 cm
0.2 cm TYPICAL
1.0 cm
0.1 cm TYPICAL

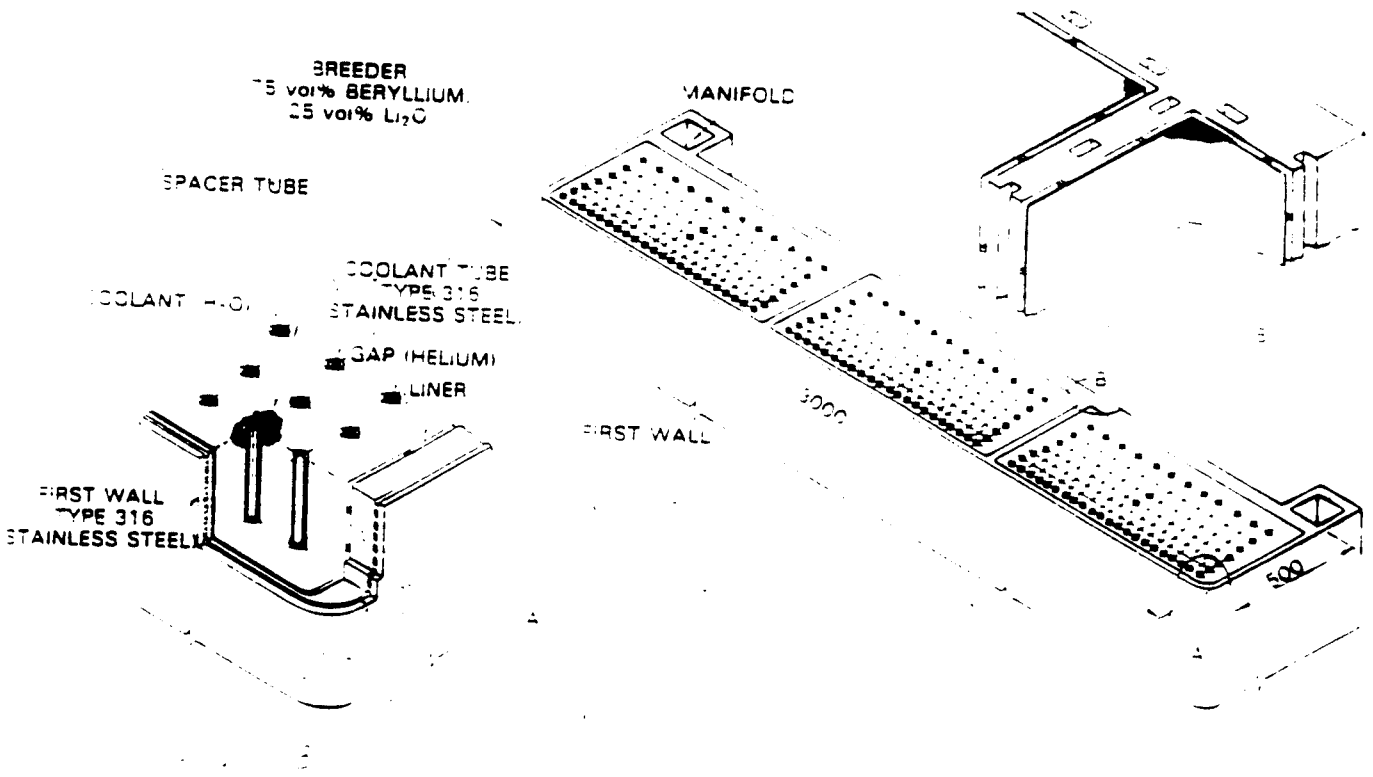
BREEDER
75 vol% BERYLLIUM
25 vol% Li_2O
SPACER TUBE
COOLANT H_2O
COOLANT TUBE
TYPE 316
STAINLESS STEEL
GAP (HELIUM)
LINER
FIRST WALL
TYPE 316
STAINLESS STEEL
MANIFOLD
FIRST WALL
3000
500

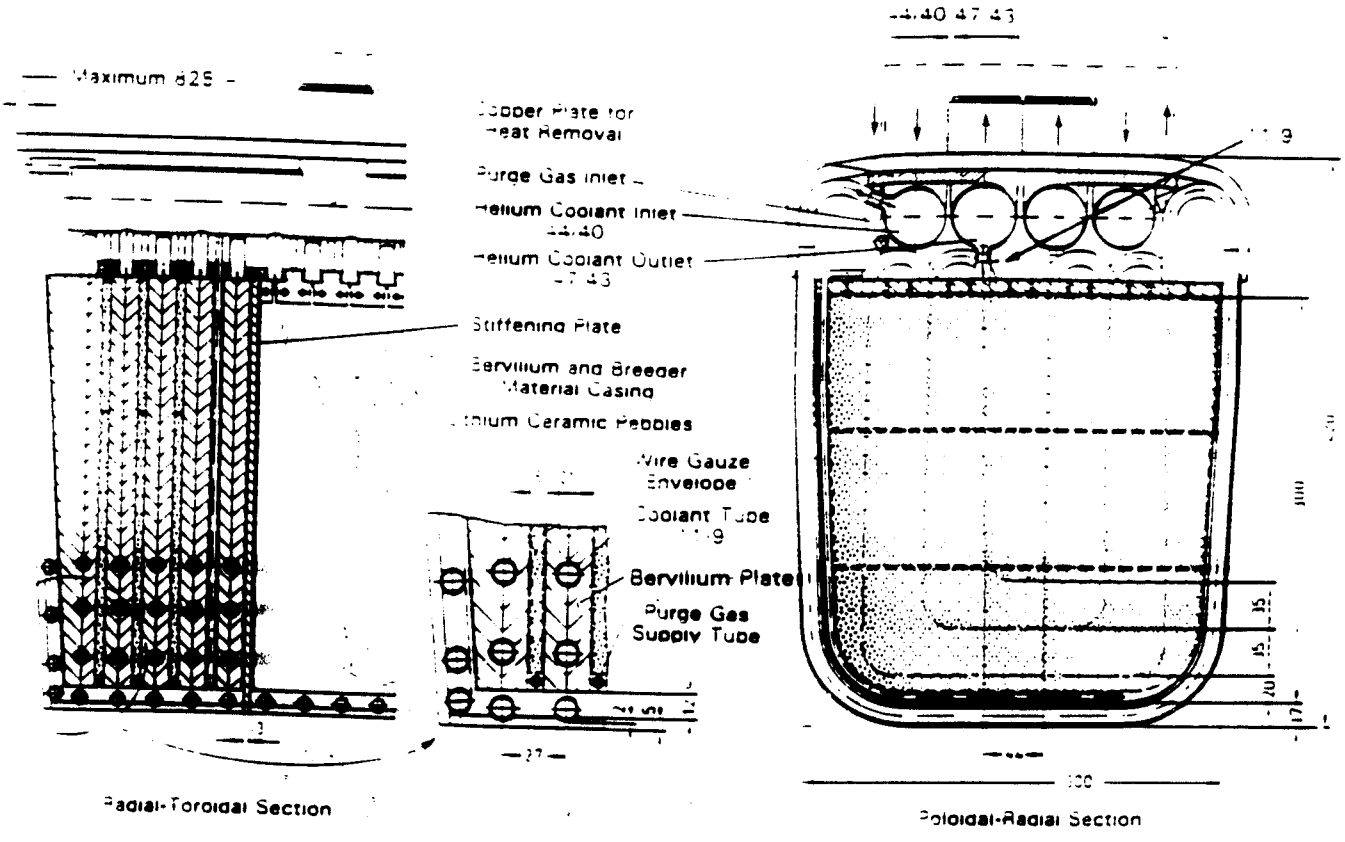

Radial-Toroidal Section

Poloidal-Radial Section

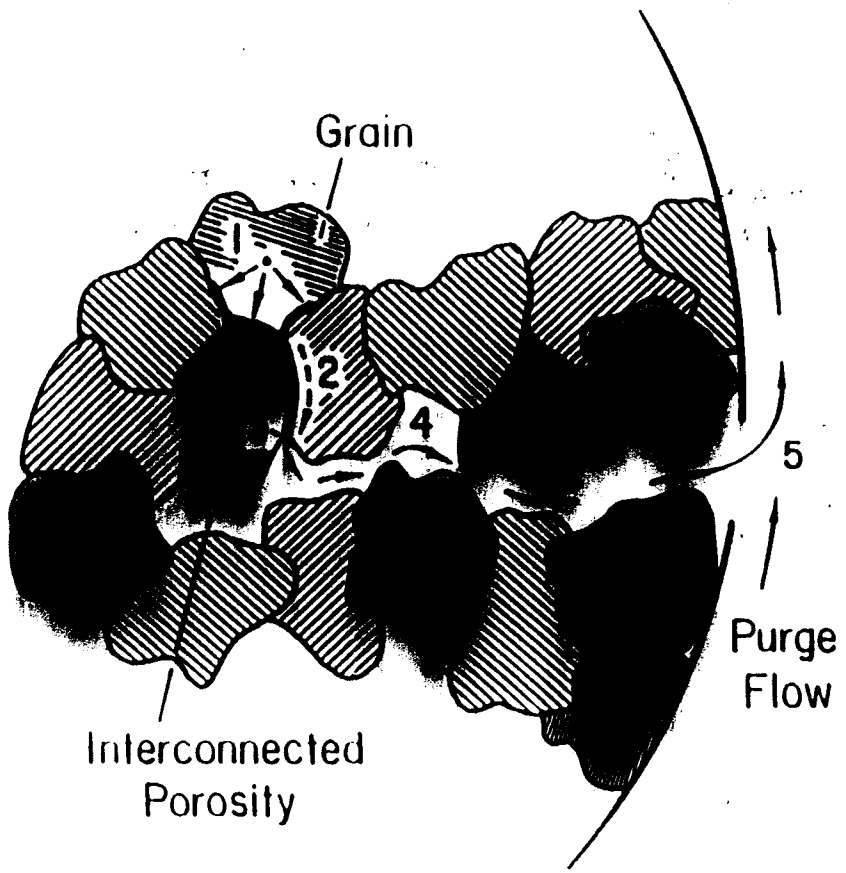

Mechanisms of Tritium Transport

1) Intragranular Diffusion
2) Grain Boundary Diffusion
3) Surface Adsorption / Desorption
4) Pore Diffusion
5) Purge Flow Convection

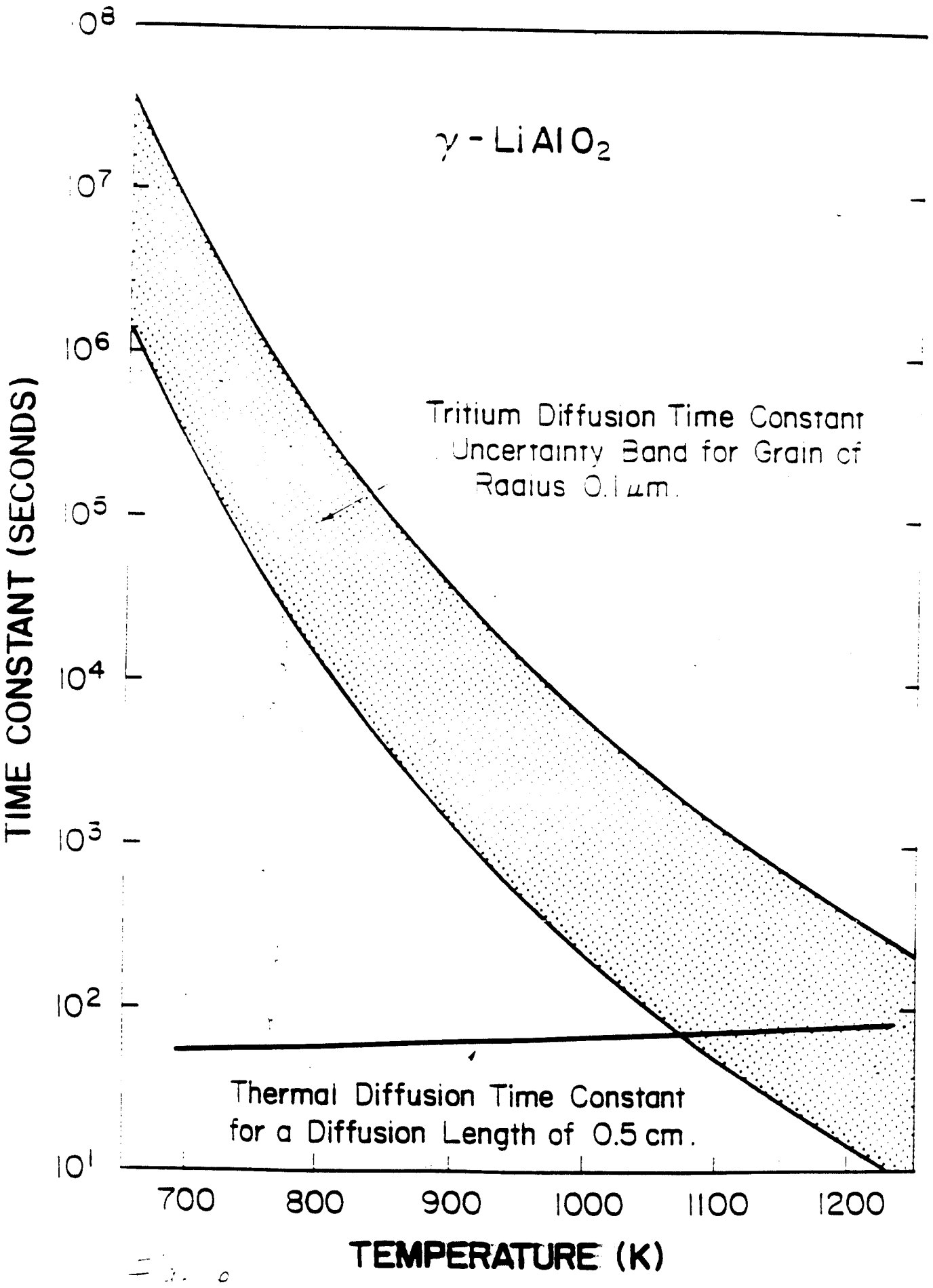
γ - $LiAlO_2$
Tritium Diffusion Time Constant Uncertainty Band for Grain of Radius 0.1 μm.
Thermal Diffusion Time Constant for a Diffusion Length of 0.5 cm.
TIME CONSTANT (SECONDS)
10^8
10^7
10^6
10^5
10^4
10^3
10^2
10^1
700
800
900
1000
1100
1200
TEMPERATURE (K)

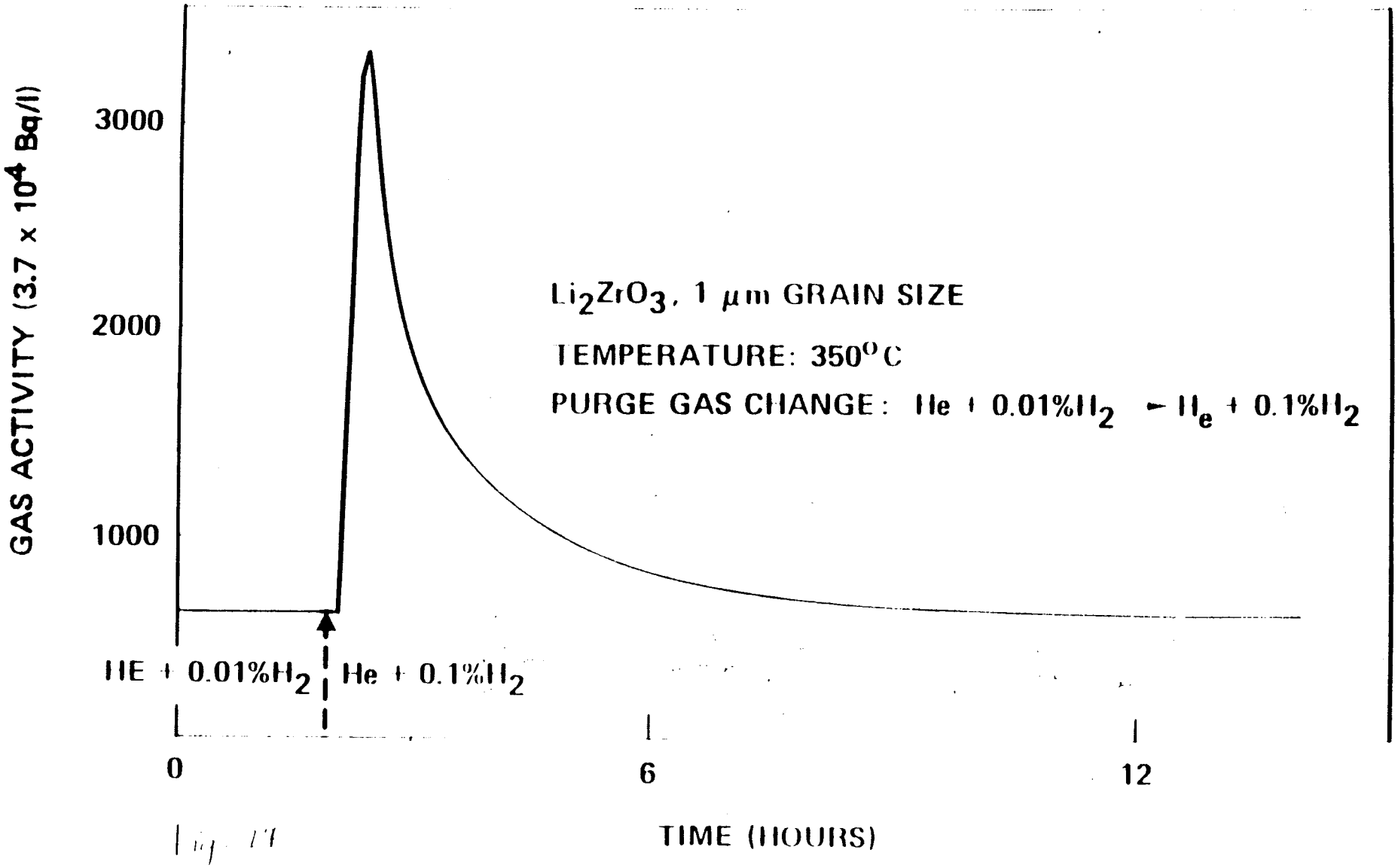
GAS ACTIVITY (3.7 x 10⁴ Bq/l)
3000
2000
1000
Li2ZrO3, 1 μm GRAIN SIZE
TEMPERATURE: 350°C
PURGE GAS CHANGE: He + 0.01%H2 → He + 0.1%H2
HE + 0.01%H2
He + 0.1%H2
0
6
12
TIME (HOURS)

Fig. 11

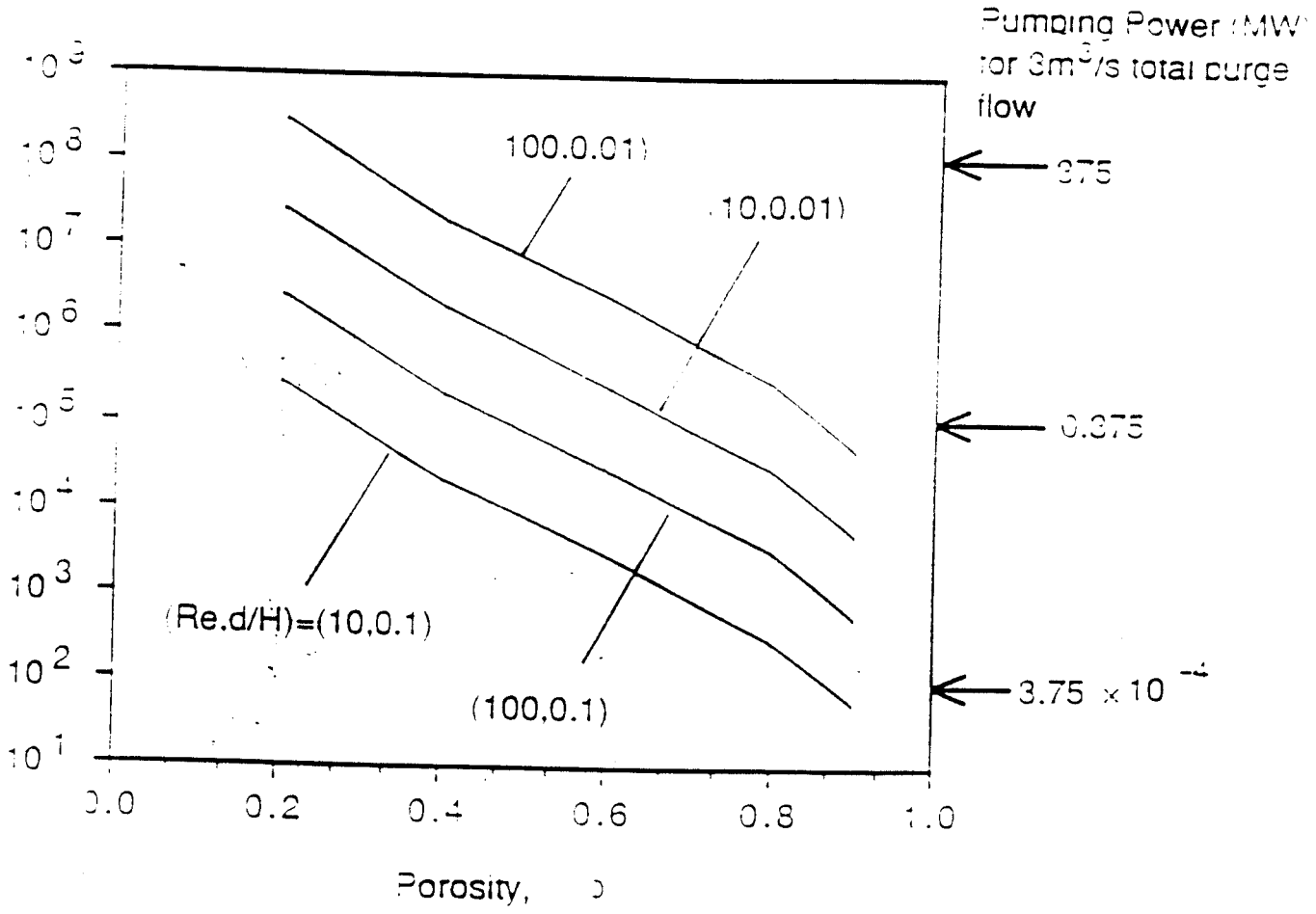
Pumping Power (MW)
for 3m³/s total purge
flow
375
0.375
3.75 x 10⁻⁴
100.0.01)
10.0.01)
(Re.d/H)=(10,0.1)
(100,0.1)
Pressure Drop (Pa)
Porosity,
0.0
0.2
0.4
0.6
0.8
1.0

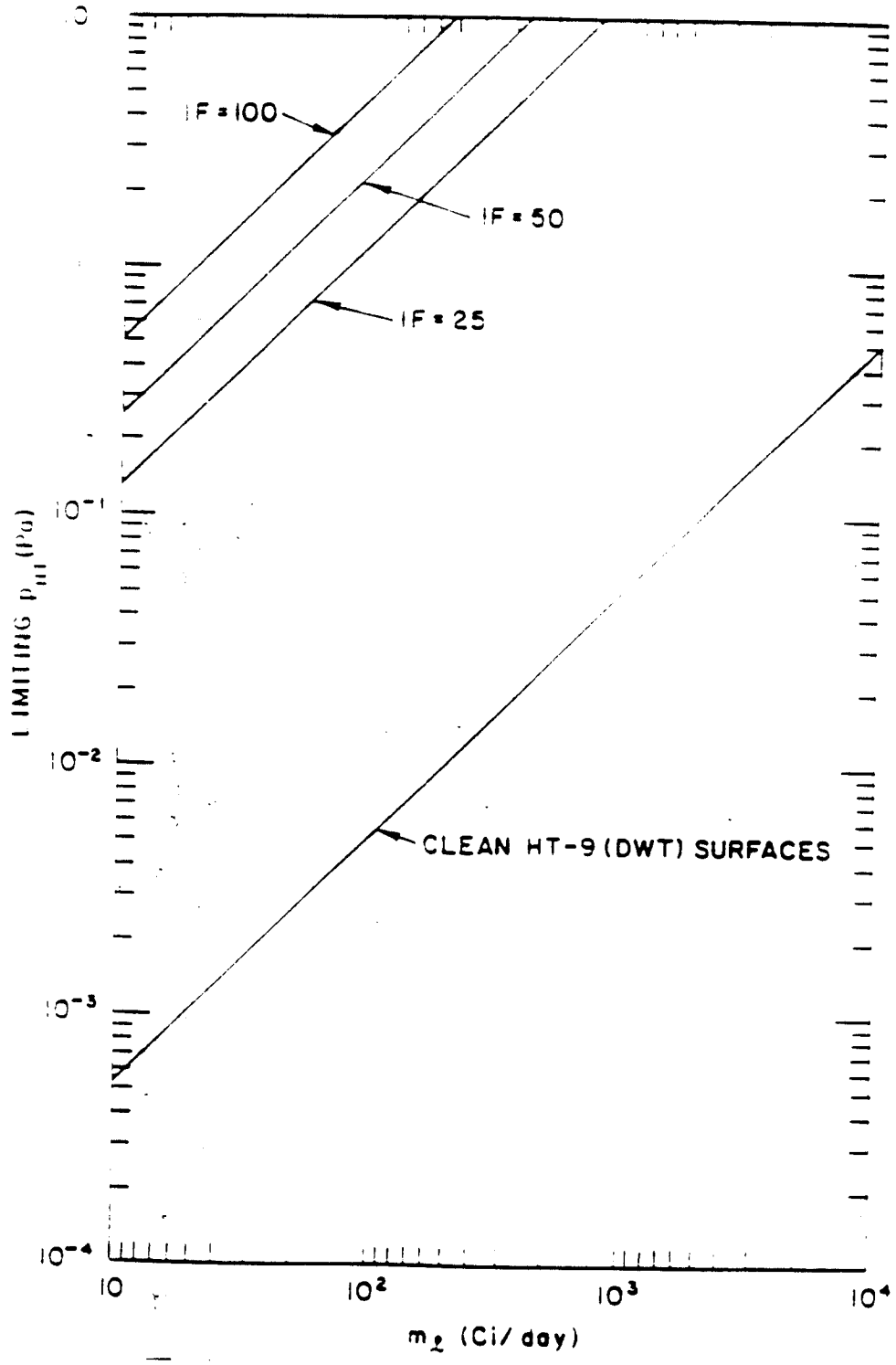
IF = 100
IF = 50
IF = 25
CLEAN HT-9 (DWT) SURFACES
LIMITING p_{III} (Pa)
10^{-1}
10^{-2}
10^{-3}
10^{-4}
10
10^2
10^3
10^4
m_ℓ (Ci/ day)

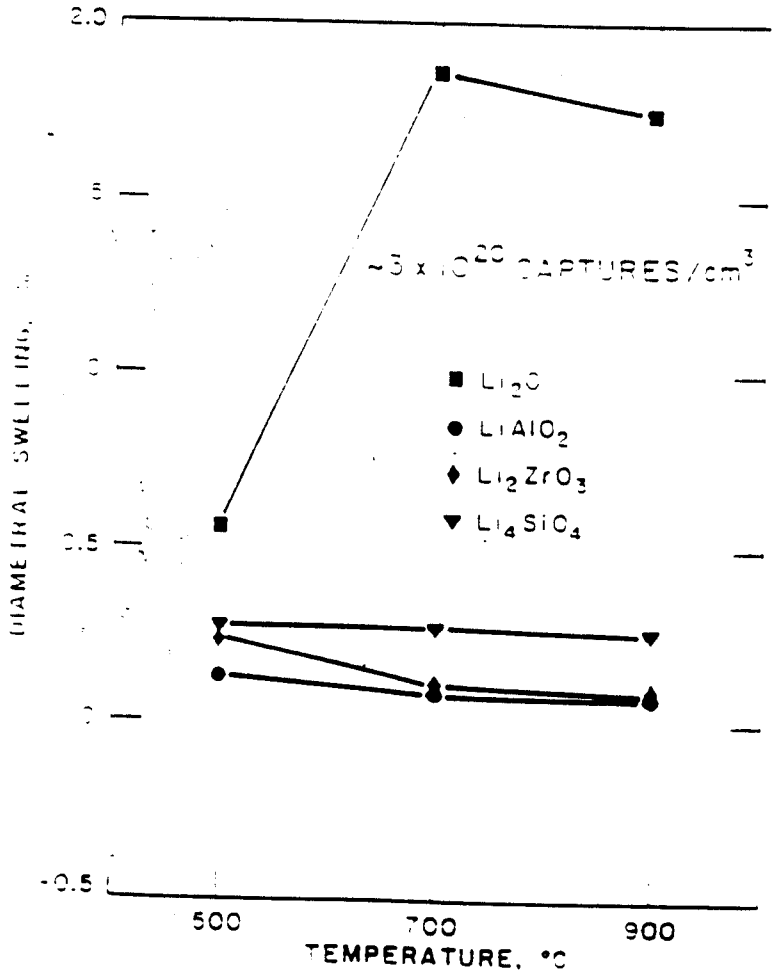
2.0
0.5
-0.5
~3 x 10^20 CAPTURES/cm^3
Li2O
LiAlO2
Li2ZrO3
Li4SiO4
500
700
900
TEMPERATURE, °C

Fig. 20

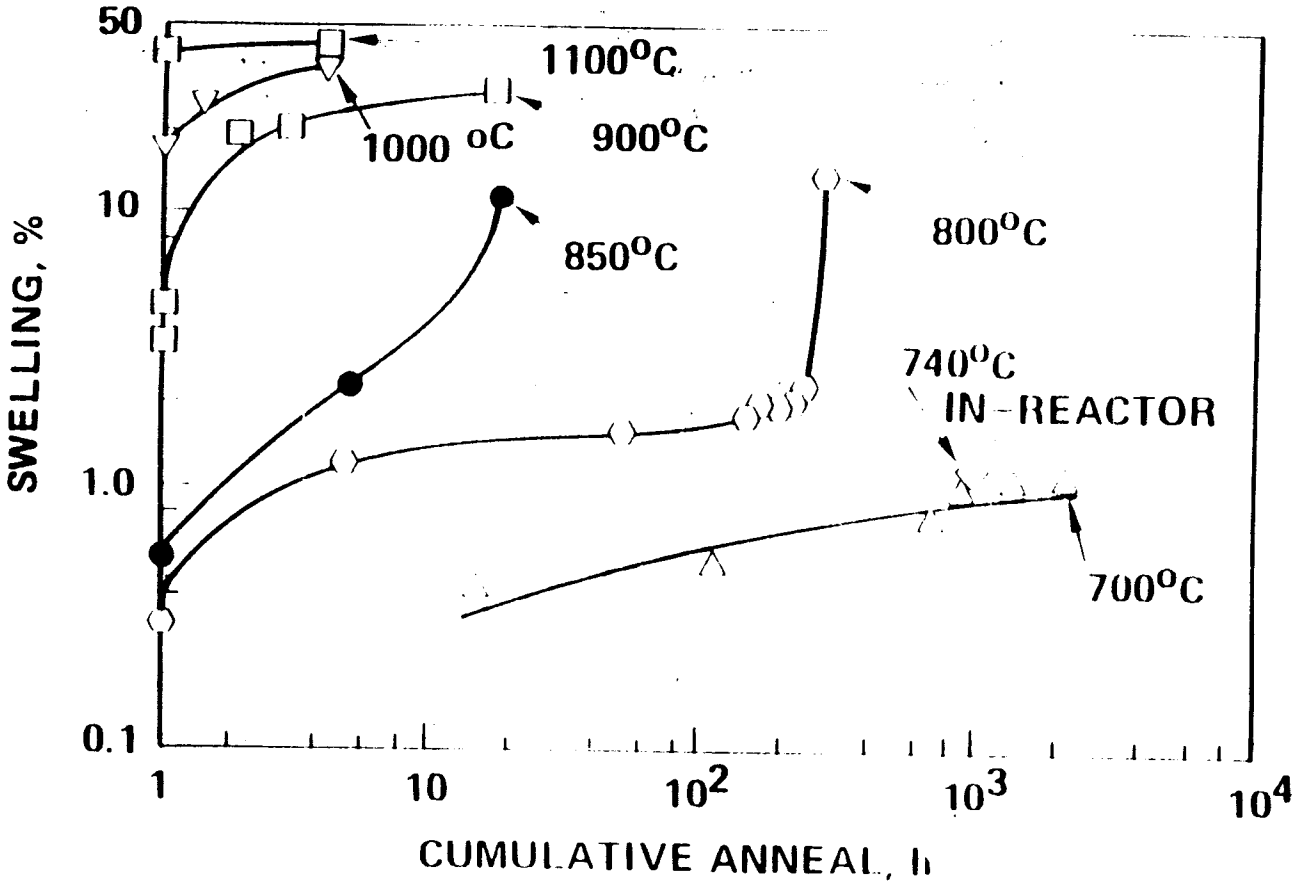
50
10
1.0
0.1
SWELLING, %
1100°C
1000 °C
900°C
850°C
800°C
740°C
IN-REACTOR
700°C
1
10
10²
10³
10⁴
CUMULATIVE ANNEAL, h

Fig. 2

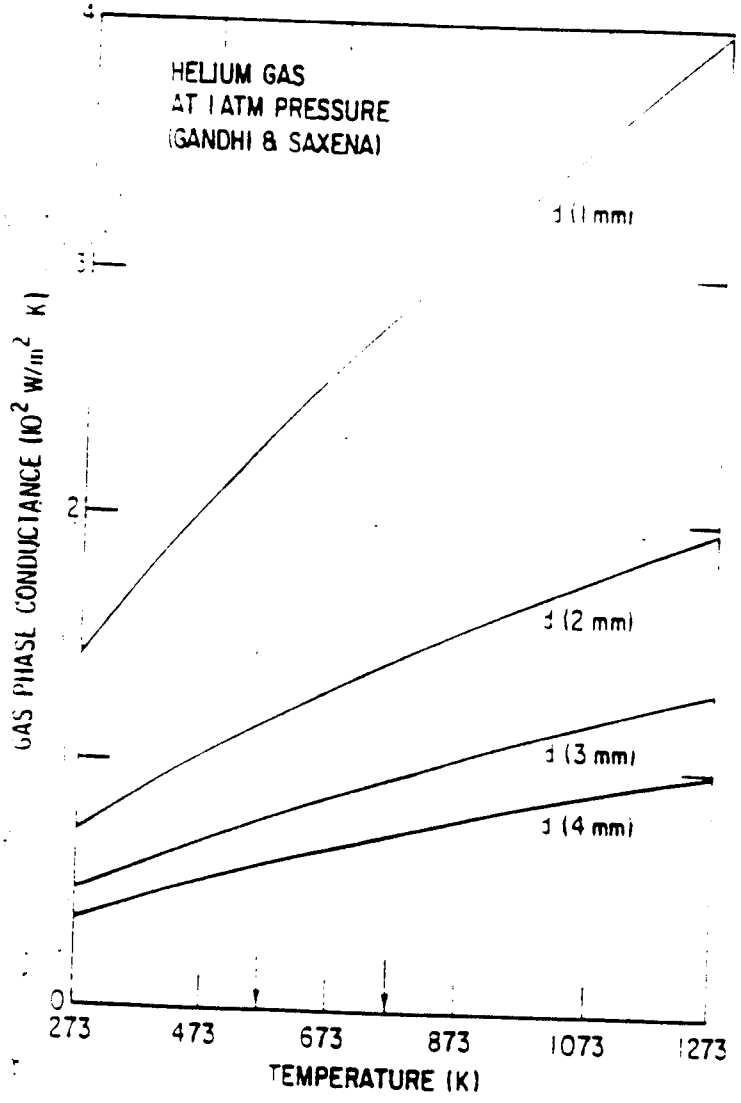
HELIUM GAS
AT 1 ATM PRESSURE
(GANDHI & SAXENA)
δ (1 mm)
δ (2 mm)
δ (3 mm)
δ (4 mm)
GAS PHASE CONDUCTANCE (10² W/m² K)
3
2
0
273
473
673
873
1073
1273
TEMPERATURE (K)

Fig. 22(a)

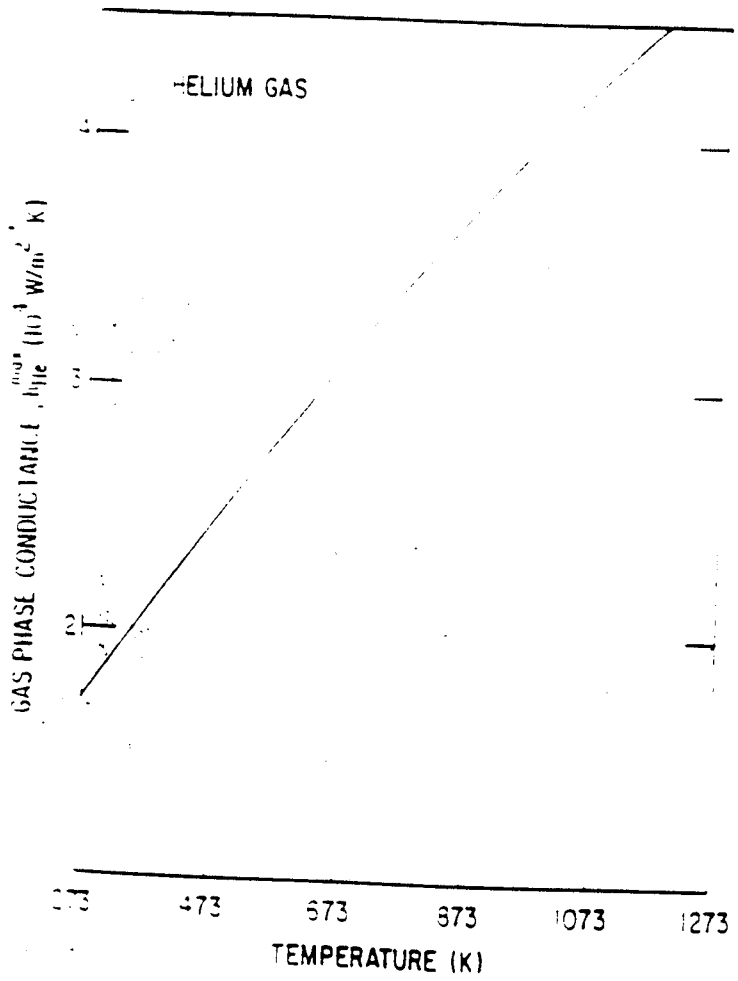
HELIUM GAS
GAS PHASE CONDUCTANCE, h_{He} (10^{-4} W/in^2 K)
473
673
873
1073
1273
TEMPERATURE (K)

Fig. 2(b)

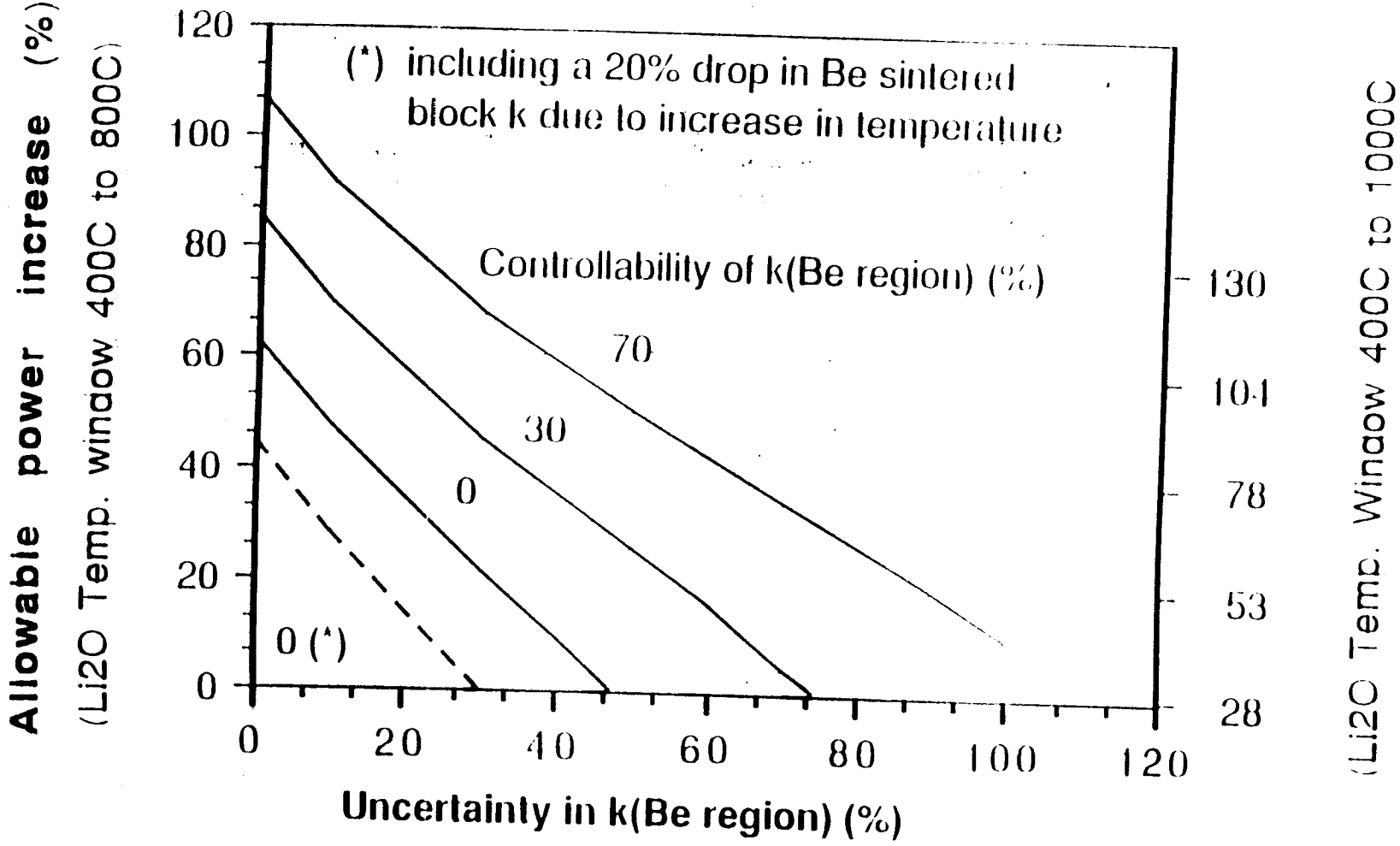
Allowable power increase (%)
(Li2O Temp. window 400C to 800C)
120
100
80
60
40
20
0
(*) including a 20% drop in Be sintered block k due to increase in temperature
Controllability of k(Be region) (%)
70
30
0
0 (*)
0
20
40
60
80
100
120
Uncertainty in k(Be region) (%)
130
104
78
53
28
(Li2O Temp. Window 400C to 1000C

Fig. 23

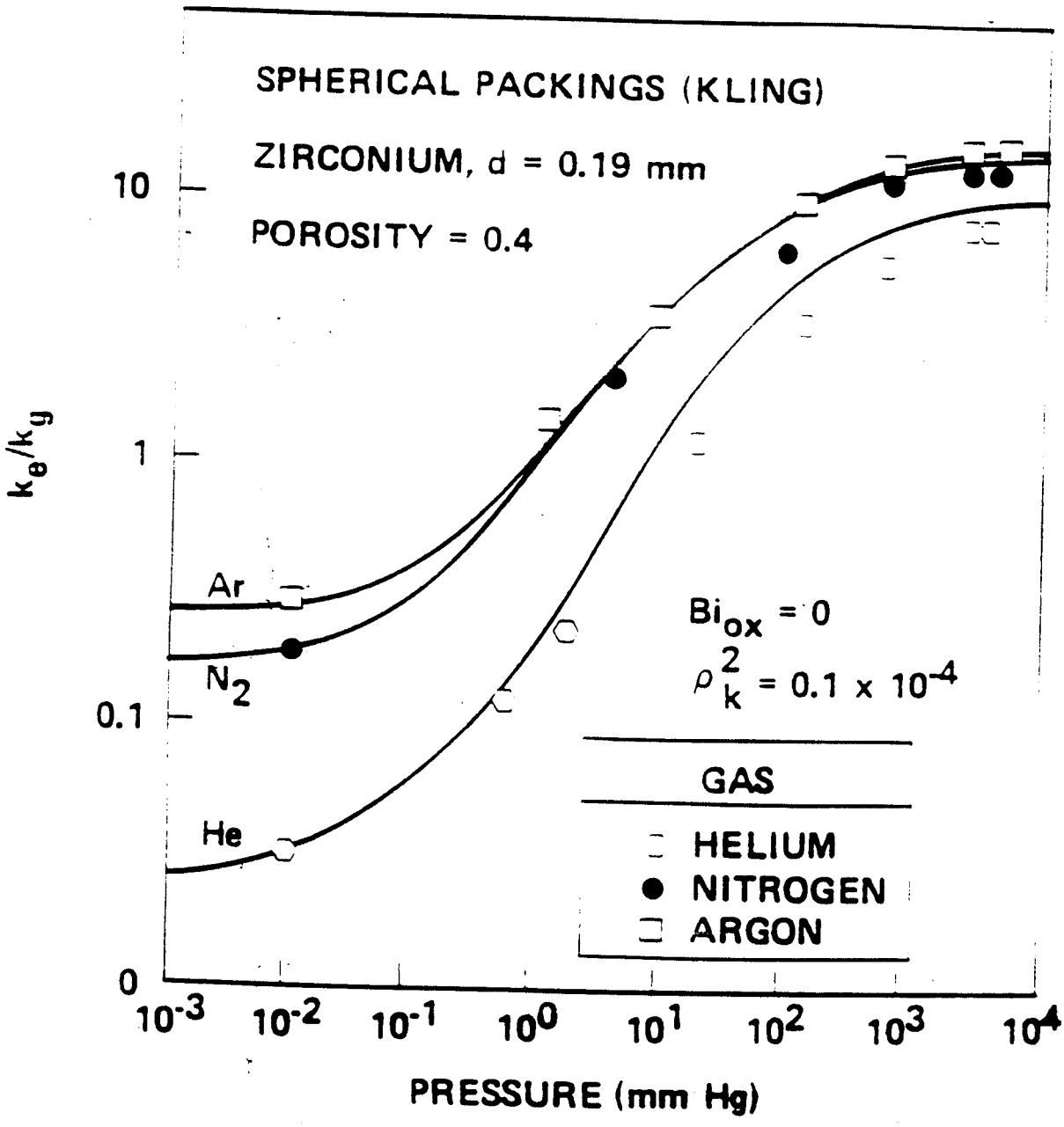
SPHERICAL PACKINGS (KLING)
ZIRCONIUM, d = 0.19 mm
POROSITY = 0.4
10
1
0.1
0
k_e/k_g
Ar
N_2
He
$Bi_{ox} = 0$
$\rho_k^2 = 0.1 \times 10^{-4}$
GAS
HELIUM
NITROGEN
ARGON
10^{-3}
10^{-2}
10^{-1}
10^{0}
10^{1}
10^{2}
10^{3}
10^{4}
PRESSURE (mm Hg)

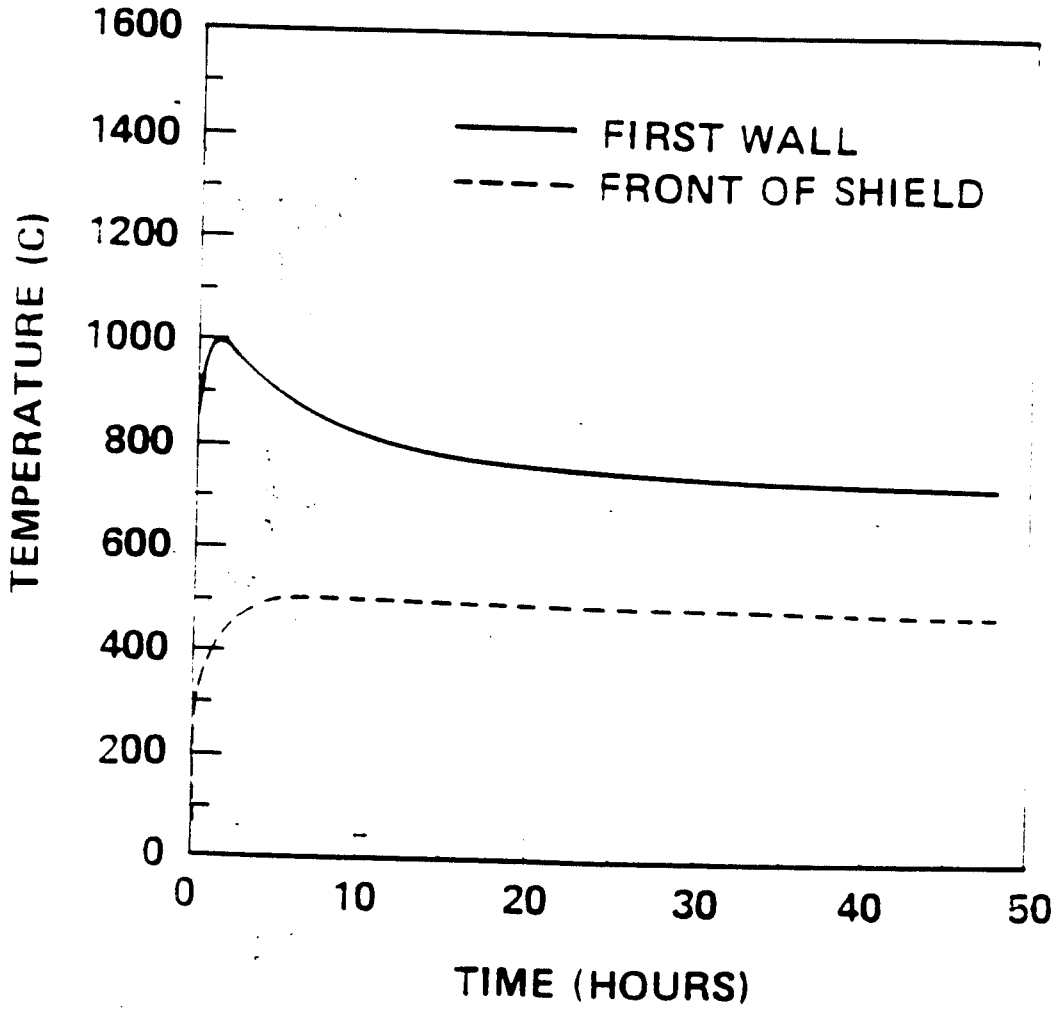
1600
1400
1200
1000
800
600
400
200
0
TEMPERATURE (C)
FIRST WALL
FRONT OF SHIELD
0
10
20
30
40
50
TIME (HOURS)

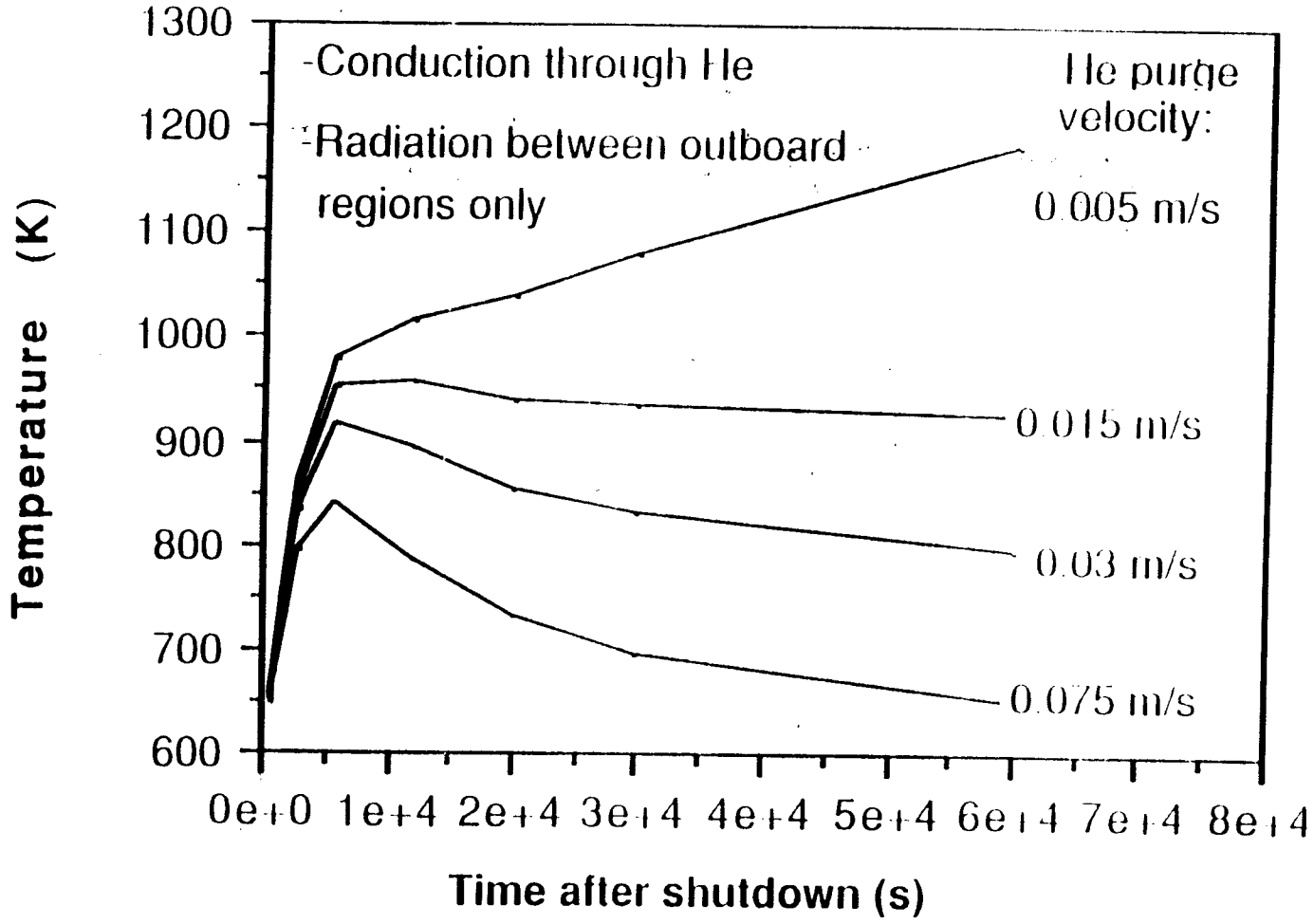
1300
1200
1100
1000
900
800
700
600
Temperature (K)
-Conduction through He
-Radiation between outboard regions only
He purge velocity:
0.005 m/s
0.015 m/s
0.03 m/s
0.075 m/s
0e+0 1e+4 2e+4 3e+4 4e+4 5e+4 6e+4 7e+4 8e+4
Time after shutdown (s)

Fig. 3.2

SOLID BREEDER BLANKET TEST PLAN

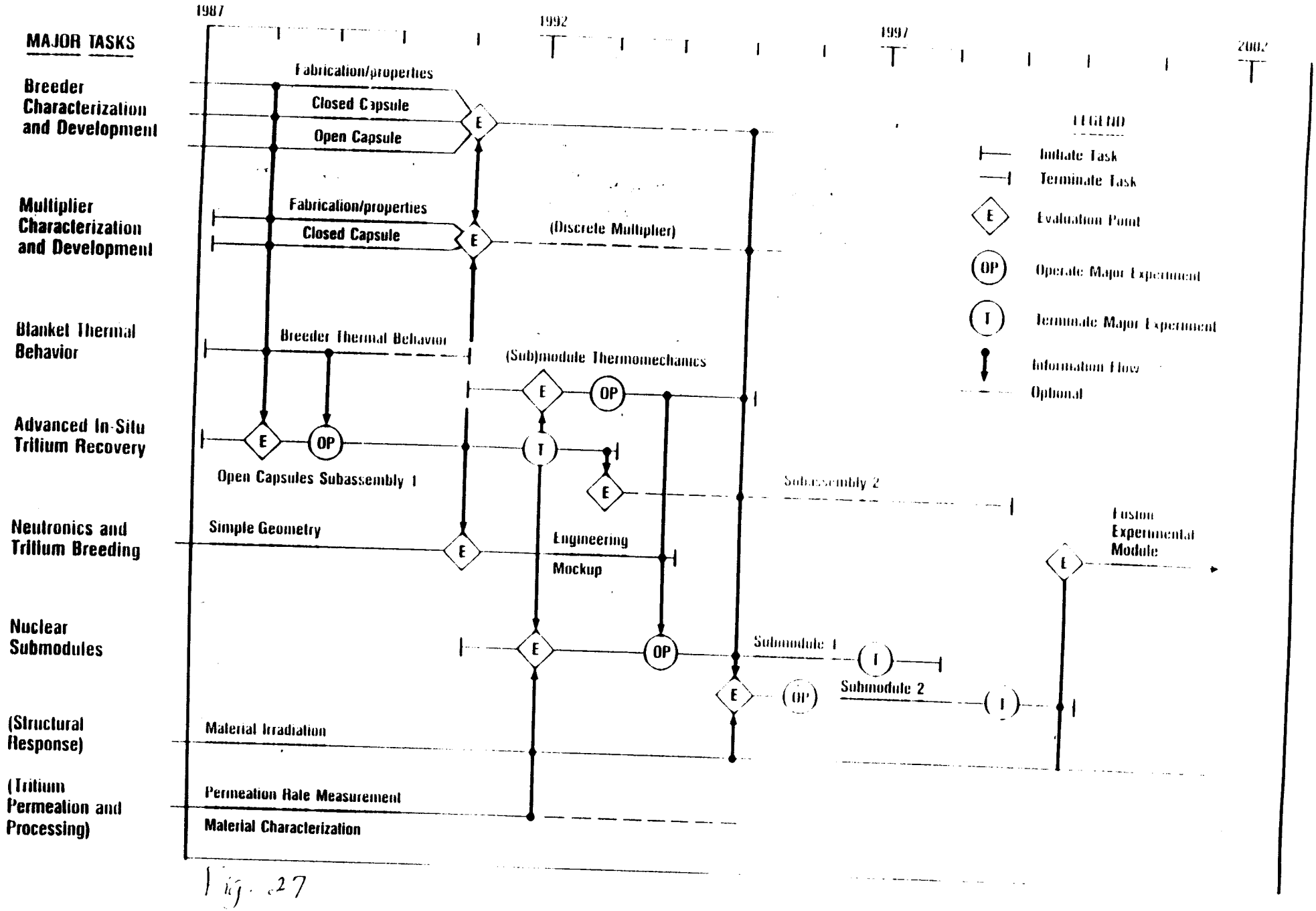

Fig. 27

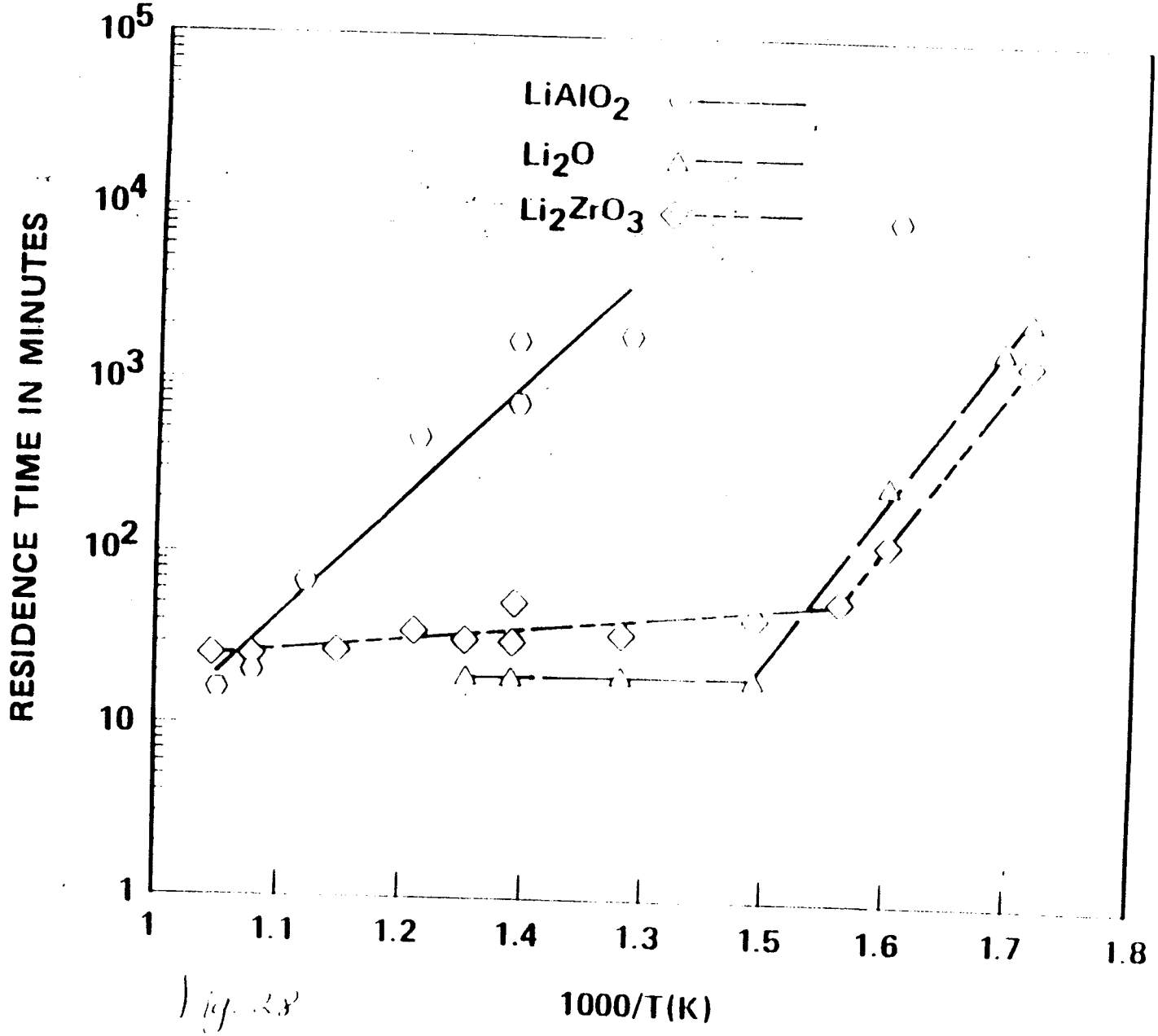
10^5
10^4
10^3
10^2
10
1
RESIDENCE TIME IN MINUTES
$LiAlO_2$
Li_2O
Li_2ZrO_3
1
1.1
1.2
1.4
1.3
1.5
1.6
1.7
1.8
1000/T(K)

Fig. 33